UNIVERSIDADE FEDERAL DE MINAS GERAIS
ESCOLA DE ENGENHARIA
PROGRAMA DE PÓS-GRADUAÇÃO EM ENGENHARIA DE ESTRUTURAS

Elissa Talma

COMPUTATIONAL AND BIOLOGICAL ANALYSIS OF THE BEST TIME TO PROCEED WITH BONE GRAFT SURGERY IN AN ADULT PATIENT WITH CLEFT PALATE

Belo Horizonte
2021

Elissa Talma

COMPUTATIONAL AND BIOLOGICAL ANALYSIS OF THE BEST TIME TO PROCEED WITH BONE GRAFT SURGERY IN AN ADULT PATIENT WITH CLEFT PALATE

Tese apresentada ao Programa de Pós-Graduação em Engenharia de Estruturas da Universidade Federal de Minas Gerais, como requisito parcial à obtenção do título de Doutor em Engenharia de Estruturas.

Área de concentração: Bioengenharia

Orientador: Prof. Estevam Barbosa de Las Casas

Coorientador: Prof. Henrique Pretti

Belo Horizonte

2021

UNIVERSIDADE FEDERAL DE MINAS GERAIS
Programa de Pós-Graduação em Engenharia de Estruturas

UFMG

ATA DA DEFESA DE TESE DE DOUTORADO EM ENGENHARIA DE ESTRUTURAS Nº: 83 da aluna **Elissa Talma**.

Às **14h** horas do dia **31** do mês de **agosto de 2021**, reuniu-se, na Escola de Engenharia da Universidade Federal de Minas Gerais - UFMG, a Comissão Examinadora indicada pelo Colegiado do Programa em **05 de julho de 2021**, para julgar a defesa da Tese de Doutorado intitulada **"Computational and Biological Analysis of The Best Time to Proceed With Bone Graft Surgery in an Adult Patient With Cleft Palate"**, cuja aprovação é um dos requisitos para a obtenção do Grau de DOUTOR EM ENGENHARIA DE ESTRUTURAS na área de ESTRUTURAS.

Abrindo a sessão, o Presidente da Comissão, **Prof. Dr. Estevam Barbosa de Las Casas**, após dar a conhecer aos presentes o teor das Normas Regulamentares passou a palavra à candidata para apresentação de seu trabalho. Seguiu-se a argüição pelos examinadores, com a respectiva defesa da candidata. Logo após, a Comissão se reuniu, sem a presença da candidata e do público, para julgamento e expedição do resultado final. Foram atribuídas as seguintes indicações:

(Aprov./Repr.)

Prof. Dr. Estevam Barbosa de Las Casas - DEES - UFMG (Orientador)_____
Prof. Dr. Henrique Pretti - Odontologia - UFMG (Coorientador) _____
Profa. Dra. Flavia de Souza Bastos – UFJF _____
Profa. Dra. Cláudia Silami de Magalhães – Odontologia - UFMG _____
Prof. Dr. Manuel Lagravere-Vich - University of Alberta _____
Prof. Dr. Diego Alexander Garzon Alvarado - Universidad Nacional _____

A candidata foi considerada APROVADA, conforme pareceres em anexo.

O resultado final foi comunicado publicamente à candidata pelo Presidente da Comissão.

Nada mais havendo a tratar, o Presidente encerrou a reunião e lavrou a presente ATA, que será assinada por todos os membros participantes da Comissão Examinadora. Belo Horizonte, 31 de agosto de 2021.

Manuel Lagravere

1) A aprovação da candidata na defesa da Tese de Doutorado não significa que a mesma tenha cumprido todos os requisitos necessários para obtenção do Grau de Doutor em Engenharia de Estruturas;

2) Este documento não terá validade sem a assinatura e carimbo do Coordenador do Programa de Pós-Graduação.

Marcelo Greco:999823316 04

To João and Enzo.

Acknowledgment

To colleagues from the University of Alberta, Silvia Capenakas, Natália Carneiro, Natália Fagundes, Fabiana Tolentino, and especially Claudine Bussolaro, who with her generosity became part of my project, helping with the reading of the data in the Dolphin program.

To dear Melisa Vélez Muriel, a Colombian friend who speaks Portuguese, very intelligent and lovely, whom I already knew virtually because we worked together on this project with the University of Colombia, but who I went to meet in person, only in Canada, was a gift that the Doctorate gave it to me, I loved meeting her and I hope this partnership will last for many projects and trips ahead.

To CAPES and CNPq. To PROPREES. To the MecBio laboratory.

All the difficulties encountered along the way, which made me persistent and strengthened me in these years.

Agradecimentos

Gostaria de agradecer ao João por todo amor, apoio e companheirismo em todas as emoções vividas por esse mundo a fora até agora, pois muitas ainda virão.

Ao Enzo, meu filho tão querido, sempre carinhoso, inteligente, colaborativo e aventureiro, sempre torcendo por mim.

A minha mãe Nires e irmã Elenne, que me apoiam em todas as decisões que tomo, sempre me ajudam, cuidam do Enzo e comemoramos juntas todas as vitórias.

Ao meu orientador Professor Estevam de Las casas, que faz parte de toda a minha trajetória na Biomecânica, desde a graduação, sempre incentivando e rompendo barreiras da interdisciplinaridade, com muita persistência, abriu as portas da engenharia para a área da saúde e para o mundo, obrigada por me permitir contribuir para a ciência, buscando novos caminhos.

Ao meu co-orientador Professor Henrique Pretti, por orientar a parte ortodôntica, contribuir com as tomografias e com o relato do caso clínico.

À Professora Soraia Mancari pelos experimentos com os animais, desde os cuidados com os camundongos até a confecção das lâminas histológicas. À técnica em análises clínica, Mara Quintela Maia, do laboratório de patologia bucomaxilofacial da UFMG, pela confecção das lâminas, as quais foram muito elogiadas, pela qualidade da confecção e coloração, pelos professores do Canadá.

Ao Professor Lagravère Vich, por me receber na Universidade de Alberta no Canadá e prestar toda assistência para mim e minha família, além de contribuir com a minha pesquisa orientando no uso dos programas de análise de imagens e em ortodontia.

Aos meus colegas do laboratório Mecbio, Mariana Pimenta Alves, Marina Las Casas, Plinio Santos, Bruna, Gabriel Rosalem, Verônica Fedotova e a saudosa Clarice Magnani, que nos deixou tão precocemente.

Aos colegas da Universidade de Alberta, Silvia Capenakas, Natália Carneiro, Natália Fagundes, Fabiana Tolentino e em especial à Claudine Bussolaro, que com sua generosidade passou a fazer parte do meu projeto, ajudando com a leitura dos dados no programa Dolphin.

À querida Melisa Vélez Muriel, uma amiga colombiana que fala português, muito inteligente e querida, que eu já conhecia virtualmente por trabalharmos juntas nesse projeto com a Universidad Nacional de Colombia, mas que fui conhecer pessoalmente, somente no Canadá, foi um presente que o Doutorado me deu, adorei conhece-la e espero que essa parceria dure por muitos projetos e viagens pela frente.

À CAPES e CNPq. Ao PROPREES. Ao laboratório MecBio.

À todas as dificuldades encontradas ao longo do caminho, as quais me fizeram ser persistente, me tornaram mais forte durante esses anos.

"A great discovery does not issue from a scientist's brain ready-made, like Minerva springing fully armed from Jupiter's head; it is the fruit of an accumulation of preliminary work."

Marie Curie

(*1867 – †1934)

RESUMO

Os pacientes com fissura palatina se beneficiam do tratamento baseado na deposição de enxerto alveolar, procedimento com taxa de sucesso muito alta em jovens. Quando o tratamento é adiado, a taxa de sucesso do procedimento diminui drasticamente. Uma causa provável para essa alteração é a ausência tanto das tensões de crescimento da criança na maxila quanto da erupção da segunda dentição, ocorrendo até os 12 anos de idade. Isso interfere na manutenção do enxerto ósseo na fissura palatina, pois o organismo entende que o enxerto ósseo colocado naquela região não é necessário, o que leva à reabsorção. A idade ideal para este enxerto ósseo é de 9 a 12 anos. Os melhores resultados foram alcançados nos casos em que o enxerto ósseo foi realizado antes da erupção do canino. Este estudo tem como objetivo utilizar simulação numérica para analisar o uso de um distrator para potencializar os resultados do tratamento do enxerto alveolar em um paciente com fissura palatina. Observar e analisar o processo de cicatrização óssea em camundongos por meio de lâminas histológicas e imagens de micro tomografia computadorizada. As imagens clínicas de um paciente foram comparadas a uma simulação de expansão palatina usando o aparelho Hyrax, com base nas CBCTs do mesmo paciente, em um modelo computacional usando o Método dos Elementos Finitos (MEF). Os dados de densidade do enxerto do paciente foram correlacionados com o módulo de elasticidade do osso para simular as condições clínicas de expansão maxilar. Os dados de densidade do enxerto foram adquiridos a partir de imagens de tomografia computadorizada de feixe cônico (CBCT) e carregados no software comercial de reconstrução automatizada Dolphin 3D e, em seguida, o modelo geométrico foi construído usando o MIMICS 20.0. Na avaliação da CBCT do paciente que não foi submetido à tração, após o enxerto, o percentual de redução do volume obtido foi em torno de 54% do enxerto em 60 dias. Nas análises do experimento com camundongos observou-se que o lado enxerto teve uma ossificação muito maior do que o lado não enxerto, devido à presença de espículas ósseas com osteócitos, e a presença de osteoblastos de enxerto ósseo originados do osso enxertado. Após a cirurgia de enxerto ósseo tardio, a expansão maxilar pode ser considerada uma opção de tratamento, causando estresse na área do enxerto em pacientes com fissura labiopalatina, pois parece atuar como estímulo positivo no enxerto ósseo. **Palavras-chave:** Fissura palatina. Enxerto ósseo. Método dos Elementos Finitos (MEF). Tomografia Computadorizada Cone Beam. Bioengenharia.

ABSTRACT

Patients with cleft palate benefit from treatment based on alveolar graft deposition, a procedure with a very high success rate in young people. When treatment is delayed, the success rate of the procedure dramatically decreases. A probable cause for this alteration is the absence of both the child's growth tensions in the maxilla and the eruption of the second dentition, occurring up to 12 years of age. This interferes with the maintenance of the bone graft in the cleft palate, as the body understands that the bone graft placed in that region is not necessary, which leads to resorption. The ideal age for this bone graft is 9 to 12 years. The best results were achieved in cases where bone grafting was performed before the canine eruption. This study aims to use numerical simulation to analyze the use of a distractor to enhance the results of alveolar graft treatment in a patient with a cleft palate. Observe and analyze the bone healing process in mice through histological slides and micro CT images. After standard cleft palate treatment, a patient's clinical images are compared to a palatal expansion simulation using the Hyrax appliance, based on the CBCTs of the same patient, in a computational model using the Finite Element Method (FEM). The patient's graft density data were correlated to the bone elastic modulus to simulate the clinical conditions of maxillary expansion. Graft density data were acquired from cone-beam computed tomography (CBCT) images and loaded into automated reconstruction commercial software Dolphin 3D and after that, the geometric model was constructed using MIMICS 20.0. In the evaluation of the CBCT of the patient who was not submitted to traction, after the graft, the percentage of reduction in the volume obtained was around 54% of the graft in 60 days. In the mice experiment analyses observed that the graft side had a much higher ossification than the non-graft side, due to the presence of bone spicules with osteocytes, and the presence of bone graft osteoblasts originated from the grafted bone. After late bone graft surgery, maxillary expansion can be considered a treatment option, causing stress in the graft area in patients with cleft lip and palate, as it seems to act as a positive stimulus in the bone graft.

Keywords: Cleft palate. Bone graft. Finite Element Method (FEM). Cone-beam computed tomography (CBCT). Computer-aided engineering.

ILLUSTRATION INDEX

TABLES

SUMMARY

1

INTRODUCTION

1.1 General considerations

The cleft lip (Fig. 1.1) is the congenital face anomaly with the highest worldwide incidence, affecting one in every 700 births (Mossey et al. 2009; Bickler et al. 2015).

Figure 0.1 Evolution of a first cleft lip surgery.
Maos (Getty Images/iStockphoto) Atlantic Center Blog

The reconstruction of the alveolar process stabilizes the dental arch, improving the periodontal support of the teeth adjacent to the fissure, assisting the phonation and promoting the

management of the bucconasal fissure. As a result, speech disorders decrease and regurgitation through the nose is avoided, improving the aesthetics and stability of the maxilla.

Most of the patients require orthodontic treatment, but the bone defect in the cleft region limits orthodontic movement, which is often necessary to perform a bone graft (Elhaddaoui et al. 2017). The reconstruction of the alveolar process is considered of fundamental importance, since it allows the permanent teeth to erupt in the restored alveolar process, making orthodontic movement possible in the reconstructed area (Bergland et al. 1986, Kalaaji et al. 1996, Jia et al. 2006).

Autogenous grafts are considered the "gold standard" materials due to their osteogenic properties, bringing together all biological principles for proper incorporation (Tanaka et al. 2008, Seifeldin 2016). An ideal bone graft material must have all of the biological principles of autogenous bone, which must be biocompatible, bioresorbable, osteoconductive, and osteoinductive. For bone substitutes, the material should be structurally similar to bone with respect to porosity and mechanical properties (Schmidt 2021).

According to Boyne and Sands 1976, a terminology to be applied for bone graft times was proposed, primary bone-grafting, when bone-grafting is performed in children less than 2 years old; early secondary bone-grafting, to be applied in patients between 2 and 5 years of age; secondary bone-grafting, when procedures are undertaken in patients between 6 and 15 years of age and late secondary bone-grafting, when the reconstruction is performed in physically mature adults.

Post graft maturation stimulation through graft remodeling is extremely important and is provided primarily by natural tooth eruption. The best age for a secondary alveolar bone grafting is during the mixed dentition stage (9-12 years), just before the eruption of the permanent canine in line with the cleft side (Eppley and Sadove 2000). After complete formation of permanent canine root, alveolar bone graft resorption is observed due to the lack of physiological stress stimulus (Feichtinger et al. 2007).

However, some patients lose the best age to undergo graft surgery and arrive at clinics looking for care when they are older. The term "late grafting" is used for grafting done when the permanent dentition is already completed (Semb, 2012).

There is a controversy in the literature regarding when is the best time to start an orthodontic movement after bone graft placement (Kazemi et al. 2002). The tooth movement is an effective stimulus that contributes for the regeneration of bone (Boyne and Sands 1976). Histological analysis studies of human biopsy showed that the graft changes from 'ground bone' characteristic and gains a standard bone appearance with the presence of trabeculae three months after surgery (Kappen et al. 2017; Rocha et al. 2012).

Therefore, most orthodontists recommend orthodontic tooth movement to the graft area after the healing period of three months. This time is ideal for the treatment of children who are still growing, but it is not so favorable for treatment in adult patients where the rate of bone resorption is high and the success rate of graft surgery is low. It is known from the literature that the application of force on bone tissue is indicated for its formation and maintenance (Carter, Dennis R., 1984; Silvana, R. et al., 2013; Stoltz, Jean-François et al.; 2018).

This stimulus is of great importance for maintaining the bone volume and preventing graft failure. As its effect to prevent excessive bone loss in patients who missed the best time for bone grafting, it is still unclear. (Uzel, Aslıhan et al, 2018). It is necessary to investigate methods to improve success in older patients.

Some authors (Bosiakov et al. 2017; Carvalho et al. 2017; Yang et al. 2012) studied tooth movement and maxillary therapies using the finite element method (FEM), a computational approach that, by avoiding clinical experiments, reduces ethical restrictions, which should be considered in an experimental approach. This method is generally used in the analysis of engineering systems and structures, in a process that involves three main steps: development of a computational model, solution of the FE model and post-processing.

In order to use the finite element method (FEM) as a technique to understand and study clinical scenarios such as maxillary expansion in cleft palate patients, it is necessary to determine the mechanical properties of the materials involved. One of the characteristics that governs the mechanical behavior of a material is its elasticity modulus. According to Kurniawan et al. 2012, the elasticity modulus of bones varies according to its type -trabecular or cortical- and its density.

One clinical case was followed, to determine the mechanical properties and obtain the CBCTs. A 27 years old patient has submitted a traditional protocol, which prepares the maxilla with the Hyrax appliance before the bone graft surgery and did not apply stresses to the graft area during the bone healing process. The software Dolphin 3D was used to assess bone grafting density and volume of this clinical case, to correlate density data of a cleft palate patient's graft to bone elasticity modulus in order to simulate clinical conditions of maxillary expansion using FEM. The clinical case CBCTs were used to reconstruct a geometrical model using MIMICS 20.0 software.

This work analyzed and compared the CBCT's of the clinical case, with 15 and 60 days after the surgery to find out how the bone absorption happens and biomechanical models simulated the use of the Hyrax orthodontic appliance to apply tension to the graft area during the bone healing process, while correcting the crossbite and maxillary expansion after surgery, to assess whether it works as a mechanical stimulus for maintaining the bone graft.

Further studies are needed to determine the ideal period to start mechanical orthodontic loading after bone graft surgery in patients with cleft lip and palate (Ochs, Mark W. 1996, Yang, Chenjie et al. 2019). Mechanical stimulation assists in bone formation and graft maintenance, preventing graft resorption. This mechanical stimulus becomes essential in adult patients who no longer have the natural biological stimulus, resulting from tooth eruption and facial bone growth.

2

MOTIVATION

The treatment of cleft lip and palate patients has a multidisciplinary character and a partnership was established between the institutions Fissured Patient Project of the Faculty of Dentistry / UFMG (Brazil), the Biomechanical Engineering Group / UFMG (Brazil), the Faculty of Dentistry of the University of Alberta (Canada) and the National University of Colombia (Colombia) to study the evolution of bone tissue after grafting and its biomechanical properties.

When the adult patients with cleft palate arrives for treatment at the UFMG dental clinic and they have not yet had a maxillary graft, they are referred to "Hospital das Clínicas", a University Hospital. The surgical procedure is always done with iliac crest bone and without use a biomaterial or another technique to try to maintain the graft in these patients who have lost the best age for the graft. It is known that the rate of resorption is high, but it is still the only treatment option for these patients.

This situation encouraged us to look for a way to assist in the success of this surgery in order to better care for these patients.

In the treatment protocol for UFMG patients, they previously use the Hyrax device, a maxillary expander, before graft surgery and the device is deactivated during and after surgery. Our proposal is that this device could be activated after graft surgery to apply tension to the bone graft area and due to the action of the load during healing, improve bone consolidation.

The proposed treatment can impact in the outcome of the procedure, favor patients who have not an efficient protocol for treatment.

With the obtained results, a better understanding of the morphological changes of the grounded bone into trabecular bone after bone graft can be possible. This expertise will assist

orthodontists to better understand the optimal timing to impose mechanical forces to induce movement during the treatment, as well as the use of palatal expanders in the post-graft phase of the bone. A biomechanical analysis of the response function of graft evolution (Dewinter et al. 2003; Peamkaroonrath et al., 2011; Erica et al. 2017), will be done in these patients.

1.2 General Objective

This study has the objective to analyze the evolution of grafted bone tissue and its mechanical properties in palatine cleft treatment to determine the optimal period to initiate orthodontic mechanical loading. It was divided into three phases:

(1) Evaluate bone graft volume and density in an adult patient using Dolphin software, to measure the bone resorption between 15 and 60 days after the surgery.

(2) An experimental animal model with male mice conducted to provide biological parameters of the process in the graft area.

(3) Computationally determine the effects of maxillary therapies under loads on the biomechanical response of an alveolar bone graft. Analyze the effect of mechanical loads on the biomechanical model of an alveolar graft with different degrees of ossification, and compare the results with a non-cleft maxilla.

1.3 Specific Objectives

1. Evaluation of the density using Dolphin software. The volume and density values found in this case can also be used in geometric modelling for finite element computer simulation.
   1.1. To evaluate the variation of volume and density of the bone graft in the maxilla of the patient with cleft palate, comparing the times of 15 days and 60 days after surgery, by means of cone-beam computed tomography (CBCT), and thus evaluate the biomechanical characteristics of the bone formed by the bone graft.
2. Evaluation of the biological bone graft healing process with male mice:
   2.1. To analyze the biological effects of the bone graft healing into the grafted cleft area.
   2.2. To relate the biological parameters of the healing process of bone graft in animals, with the biomechanical parameters of the patient bone healing, such as volume and density, found in the analysis of CBCTs, using the Dolphin.

3. Analysis based on the CBCT images from the patient:

    3.1. To modeling of the maxilla from computed tomography data of the patient before and after bone grafting;

    3.2. Clinically analysis, through computed tomography and image superimposition, of bone tissue evolution and its mechanical properties after secondary grafting;

    3.3. Evaluation of the level stress levels generated by the movement, using finite element method analysis. An appropriate representation of the chewing loading will be used for the simulation of bone tissue evolution at the bone graft site and its mechanical properties.

3

LITERATURE REVIEW

3.1 Cleft Lip and Cleft Palate

Cleft lip and cleft palate represent one of the most frequent orofacial congenital anomalies, with a multifactorial etiology, involving genetic and environmental factors (Kawalec et al. 2015).

Dixon et al. 2011 analyzed the cause of the birth with cleft lip and palate babies and founded that clefts of the lip and/or palate (CLP) are common birth defects of complex etiology. CLP can occur in isolation or as part of a broad range of chromosomal, Mendelian, or teratogenic syndromes.

Fissures affect the middle third of the face and are caused by non-fusion of maxillary bones during the sixth and tenth weeks of intrauterine life. The most commonly used classification of cleft lip palates by professionals is that of Spina, which groups the fissures according to their location and with the structures (Spina 1973).

It is known that a high prevalence of agenesis, which is a genetic absence of some teeth, supernumerary teeth that are beyond the normal number of teeth, and dental crown shape changes are common features present in the oral cavity of these individuals and can be considered part of the individual phenotype (Tannure et al. 2012).

Cleft lip and cleft palate may be associated with syndromes and often have dental arch malformation. The rehabilitation process of these patients begins at birth and extends to adulthood, aiming at aesthetic and functional improvement, as well as their social reintegration (Kappen et al. 2017).

Cleft lip and cleft palate patients undergo multidisciplinary treatments for a long time due to their clinical complexity. The orthodontic treatment is usually essential in the rehabilitation of

these patients; however, the alveolar bone defect present in the region of the fissures that surround the alveolar ridge limits the possibility of tooth movement, making the bone graft a fundamental procedure mainly in the time of the mixed dentition (Silva Filho et al. 2013).

An interdisciplinary team approach is highly recommended to accurately diagnose and to properly customize a treatment plan. The general roles of medical, dental, and related healthcare providers will be highlighted, with a specific emphasis on dental treatment (Lee et al. 2014) (Table 3.1.1).

Table 3.1.1 Roles of Healthcare Providers in the Longitudinal Treatment of Cleft (Lee, Cameron CY et al.,2014)

Provider	Role
Cleft surgeon: oral and maxillofacial surgeon, plastic surgeon	•Cheiloplasty •Palatoplasty •Maxillary expansion •Alveolar bone grafting •Orthognathic surgery •Revision surgery •Cosmetic procedures when indicated
Orthodontist	•NAM •Standard orthodontic treatment
Pediatric and/or general dentist	•Patient education •Manage alterations in primary and secondary dentitions •Reinforce oral health habits
Prosthodontist	•Placement of dental prostheses
Periodontist	•Monitor periodontal health •Gingival grafting
Otolaryngologist	•Manage neonatal airway •Placement of tympanostomy tube •Monitor middle ear effusion and hearing loss •Manage airflow obstruction
Speech-language pathologist	•Speech therapy

3.2 Bone tissue healing

Bone tissue is permanently renewed throughout life and at least three specialized bone cells are needed for the synthesis, modeling and remodeling of this tissue: osteoblasts, osteocytes and osteoclasts. The cells responsible for bone formation activity are the Osteoblasts, which synthesize the organic part of the bone matrix, for the matrix maintenance and activity the osteocytes are essential, and osteoclasts, which are large multinucleated cells responsible for the dissolution and absorption of the bone, together with osteoblasts participate in constant bone turnover and remodeling. The phenomenon of bone regeneration is highly complex and comprises a series of successive mechanisms, Junqueira 2004.

According to Guyton and Hall 1997, bone deposition is partially regulated by the level of the stresses imposed on the bone. Bones under higher tension and greater curvature present more active osteoblasts, thus becoming stronger and more resistant then bones not subjected to tension.

According to Nordin and Frankel 2001, histologically there are two types of bones: lamellar bone and non-lamellar bone. Primary or non-lamellar bone tissue is less mineralized and is considered immature bone. This type of bone is found in the growing bone metaphysis region and in the callus, as well as in some bone pathologies. In adults it is uncommon, persisting only close to the skull bone sutures, dental alveoli and at some tendon intersection points. Secondary or lamellar bone tissue replaces non-lamellar bone and is usually found in adults.

The relative amount of each type of bone, the number, thickness and orientation of the bone trabeculae depend on the forces to which the bone is exposed (Nordin 2001). In countless situations, bone tissue has the ability to recover. However, vascularization failures and mechanical instability may influence the extent, speed and quality of repair, making it difficult or even preventing proper bone repair (Pinheiro et al. 2006).

The phenomenon of bone regeneration is highly complex and comprises a series of successive mechanisms (Junqueira 2004). Whenever the continuity of a bone is interrupted, whether by a traumatic, pathological or surgical injury, a sequence of reactions is immediately established to fill the lesion space. Commonly, when a fracture occurs, there is laceration of the periosteum and endosteum, and blood vessels from bone and adjacent soft tissues rupture, blood leaks and

a clot or hematoma forms in and around the fracture site, and immediately the adjacent bone, by indirect injury, becomes necrotic (Carano and Filaroff 2003; Doblaré et al. 2004).

In the early stages of acute inflammation, the blood clot can still be recognized between the medullary cavities and between the fractured ends, acting as a fibrin framework that facilitates the repair cell migration. Later, this clot will be replaced by granulation tissue that will become progressively more fibrous (Dobleré et al. 2004).

Simultaneously, the osteogenic cells of the endosteum also proliferate, developing a ring or a connective collar around the fragments, called bone callus. The callus (external) is the callus that forms around the extremities, while the callus (internal) is the callus that forms between the bone fragments (Dobleré 2004; Chakkalakal et al. 1999). The bone shape is reshaped to allow functionality and restore normal or at least close to normal resistance (Junqueira 2004).

Because it is a self-healing tissue, its properties and geometry are altered in response to changes in mechanical demand, adopting an atomic disposition regarding the tensions or mechanical stimuli to which the bone is subjected (Nordin and Frankel 2001).

3.3 Orthodontic Treatment

The orthodontic treatment of patients with clefts follows the following protocol: pre-graft orthodontic intervention; secondary alveolar bone graft, orthodontic post-graft intervention; orthognathic surgery; finalization and containment (Kappen et al. 2017, Rocha et al. 2012).

Orthodontic intervention before the bone grafting prepares the region to receive the autogenous spongy bone graft removed from the iliac crest, allowing dental movement in the restored region. After surgery, it is up to the orthodontist, if the canine tooth has not yet erupted, to observe the eruption of the dental element through the graft. If the canines are already erupted, corrective orthodontics can be started within 60 to 90 days after surgery.

After orthodontic intervention and if necessary after the end of patient growth, orthognathic surgery can be performed (Johanson and Ohlsson 1961). Orthognathic surgery for the treatment of maxillomandibular deformities is usually applied after bone growth ends. It is performed to

correct conditions of the maxilla and mandible, related to skeletal disharmonies and dental bite problems that cannot be easily treated with an orthodontic appliance.

The most recent articles related to orthodontic movement in the graft area of patients with cleft palate as Sun et al. 2018, show that the application of force soon after grafting surgery stimulates bone formation and decreases resorption in patients that missed the appropriate treatment time.

Sun et al. 2018, analyzed the biological effects of orthodontic tooth movement into the grafted alveolar cleft area. An animal model of orthodontic tooth movement into the grafted alveolar cleft area was established in 8 week old Spregue-Dawley rats. The animals were divided into the experimental group and the control group. They were observed before orthodontic stimuli; 1 day, 3 days and 5 days after orthodontic stimuli. The collagen fibers and the activities of the osteoclasts and osteoblasts were evaluated by histologic staining.

The results showed significant differences between the groups, suggesting that the orthodontic treatment after bone graft surgery in patients with cleft lip and palate can strengthen the bone reconstruction process owing to the mechanical pressure from the orthodontic stimuli, inducing bone resorption and subsequent bone deposition. (Figs. 3.1 and 3.2).
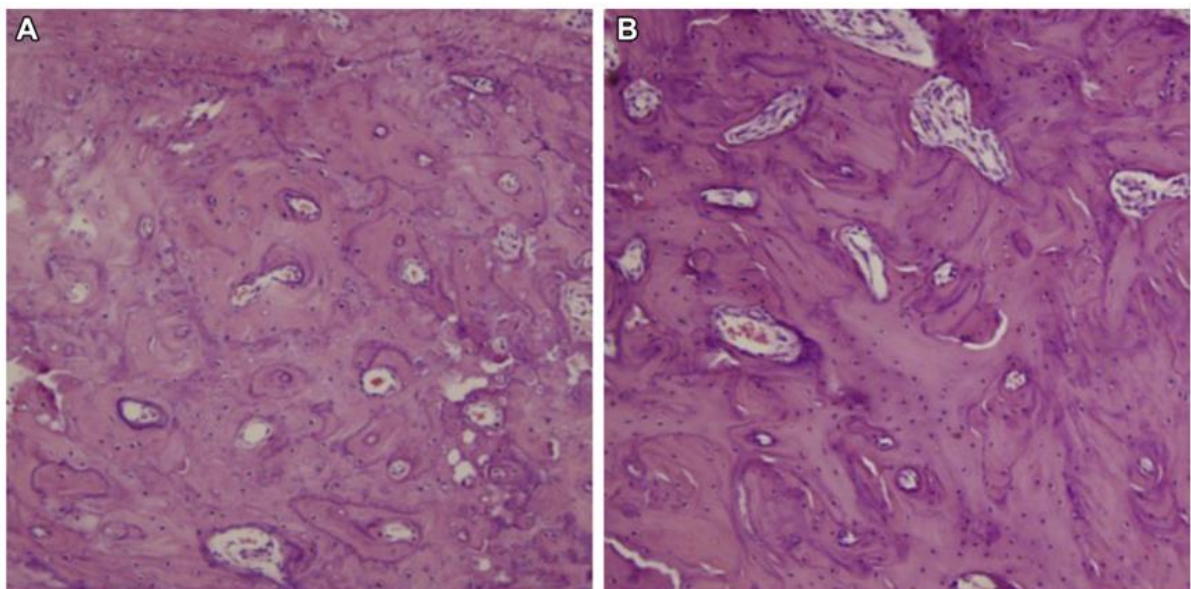
Figure 0.1 Bone tissue in bone graft area 1 day after orthodontic stimuli: control group (A) and experimental group (B) (hematoxilin and eosin - HE staining, original 100 X magnification). Sun et al. 2018.
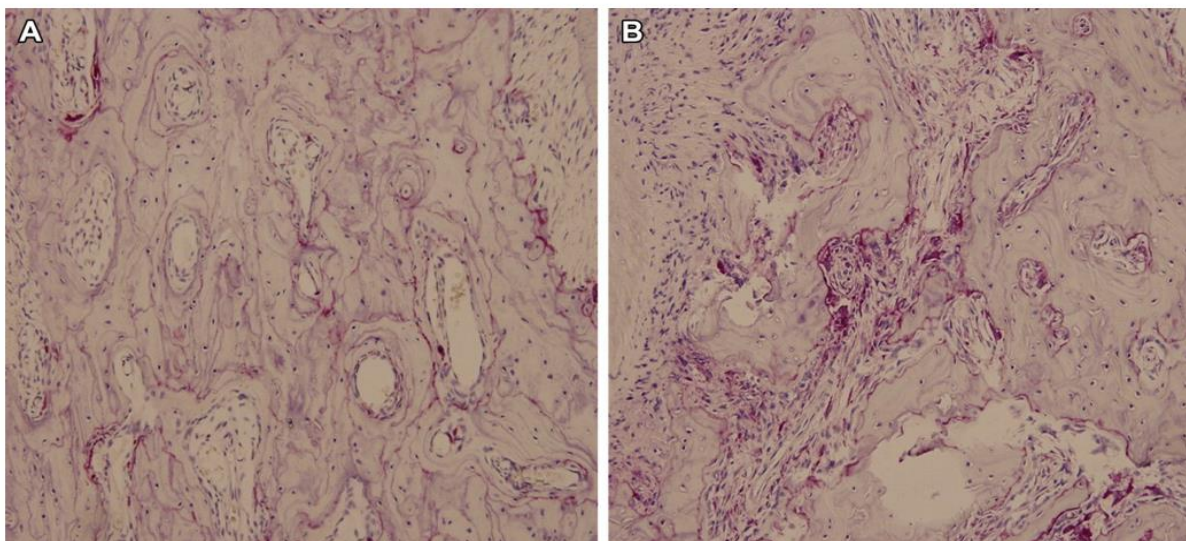
Figure 0.2 Tartrate-resistant acid phosphatase staining of bone graft area 3 days after orthodontic stimuli: control group (A) and experimental group (B) (original 100 X magnification). Sun et al. 2018.

Uzel et al. 2018, tested the post-graft stimulation of the maxillary expansion with a Quad-helix appliance (Fig.3.3) in patients with cleft lip and palate who missed the appropriate treatment time. Thirty patients in permanent dentition with unilateral cleft lip and palate were divided into two groups. In Group I, slow maxillary expansion was performed before secondary alveolar bone grafting and in Group II, slow maxillary expansions were performed six weeks after secondary alveolar bone grafting. The bone graft volume loss was significantly higher in Group I than in Group II after 6 months of healing, and the increase in bone density was significantly higher in Group II than in Group I after the same period. In the permanent dentition stage, starting slow maxillary expansion 6-8 weeks after secondary alveolar bone grafting may be a treatment of choice to stimulate the bone graft area.

Figure 0.3 Quad-helix appliance in mouth. Uzel et al. 2018.

3.4 Bone Graft

Secondary bone graft was first described in 1972 by Boyne and Sands, and since then, it occupies an important position for the treatment of patients with cleft lip and palate.

Boyne et al. 1976, stated that it is generally well accepted that definitive dental rehabilitation of patients with anterior palatal and alveolar clefts has been less than satisfactory because of the failure to solve the basic problem of lack of osseous support in the cleft area. Even with the sophistication of modern practice, orthodontic, prosthodontic, and routine dental care in patients with such defects has been difficult. They also wrote that the prognosis of dental rehabilitation without appropriate bone-grafting procedures of the alveolar and pre-palatal cleft is unfavorable. According to Boyne, secondary bone-grafting is when procedures are undertaken in patients between 6 and 15 years of age and late secondary alveolar bone-grafting, when the maxilla reconstruction is performed in physically mature adults.

Steen et al. 1985, compared the treatment results after secondary and late secondary bon-grafting in 293 cleft-palate patients and concluded that the best results are seen in the youngest group of patients immediately before eruption of the canine in the cleft-region.

The morphological rehabilitation of the fissured individuals involves plastic surgery, in the first months and years of age, to repair the defect in the soft tissue, lip and palate, leaving a residual alveolar fissure that should be treated with bone graft in the future. The main difference in the treatment protocol of the various rehabilitation services is the moment of the bone graft. According to the time of occurrence, the bone graft can be considered primary, secondary or tertiary (late) (Kappen et al. 2007).

Eppley et al. 2000, revised many articles and concluded that bone grafting of the alveolus is an essential step in the reconstruction of the orofacial cleft deformity. Secondary grafting with iliac marrow consistently produces trabecular bone to unify the maxilla. The high success of this procedure makes it the preferred at most centers to prevent maxillary segmental collapse.

The autogenous bone graft in these patients, considered a "gold standard" in the treatment, is often recommended close to the eruption of the permanent canines, in an attempt to guide this dental element, guaranteeing support to the teeth near the site of the cleft. The ideal time for post-graft orthodontic movement is still discussed in the literature (Kazemi et al. 2002).

Autogenous bone grafting has several advantages over other augmentation techniques including short healing times, favorable bone quality, lower material costs, no risk of disease transmission or antigenicity (Misch 2010). It is the only graft material with osteogenic properties that can directly form bone. Bone cells, in higher concentration in the cancellous marrow, surviving the transplantation produce new bone. Osteocompetent mesenchymal cells are transformed into osteoblasts through osteoinduction.

Regarding the development of potential bone graft alternatives, autologous bone graft remains the gold standard of care for treatment of bone defects (Schmidt 2021).

Silva et al. 2000, in a longitudinal analysis of 50 cleft palates patients' radiographs, emphasized the importance of performing the secondary bone graft in order to guide the spontaneous eruption of permanent canines. They observed that, in 72% of the analyzed patients submitted to the secondary graft, the canines erupted without the necessity of surgical procedures. In addition, they observed that the grafted bone filled the region of the cleft present in the alveolar region and joined the adjacent bone, which could be seen radiographically after a mean period of 3 months.

According to Bergrand et al. 1986, the optimal age for this secondary bone grafting has been found to be from 9 to 11 years. The best results have been achieved in cases where the bone graft was carried out prior to the eruption of the canine. No significant difference between unilateral and bilateral cases was found. When the same procedure was carried out after eruption of the canine, the results were less favorable.

Shirota et al. 2010, measured the bone volume necessary for secondary bone grafting (Fig.3.4) in the alveolar cleft using surgical simulation software based on three-dimensional computed tomography in patients with cleft lip and palate to compare with the actual volume used and to evaluate the consistency. They concluded that the estimation of the bone volume necessary for the repair can be estimated by analyzing cone-beam computer tomography (CBCT) scan data and image analysis software taken 1 month before the surgery.
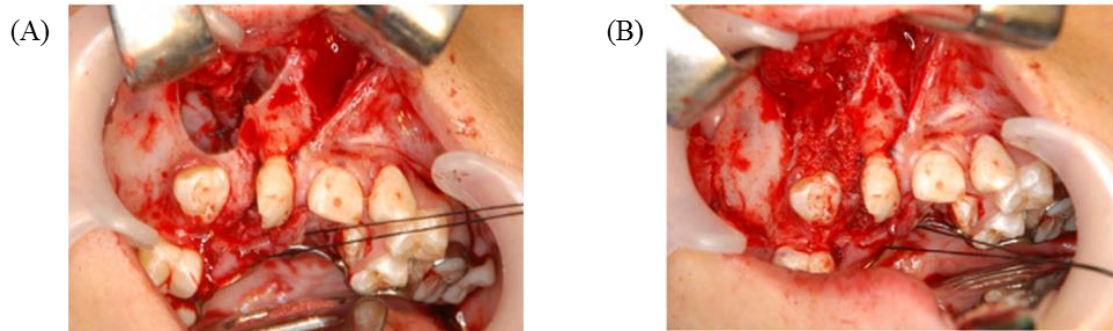
Figure 0.4.1 Surgical procedures for bone graft in the patient with cleft palate.
(A) Reconstruction of nasal layer from upturned flaps. (B) The alveolar bone defect is packed firmly with cancellous bone and marrow. Shirota et al. 2010.

Luque-Martín et al. 2014, reviewed 104 cases of alveolar graft (Fig.3.5) in the cleft lip and palate patient showed that 70% of the patients underwent the procedure before the age of 15 (median 14.45 years); 70% of the graft patients underwent pre-graft maxillary expansion. A total of 100 cases were recorded as successful (median age of 14.58 years, 68 underwent pre-graft expansion) and only 4 were recorded as failures (median age of 17.62 years, 3 underwent pre-graft expansion).
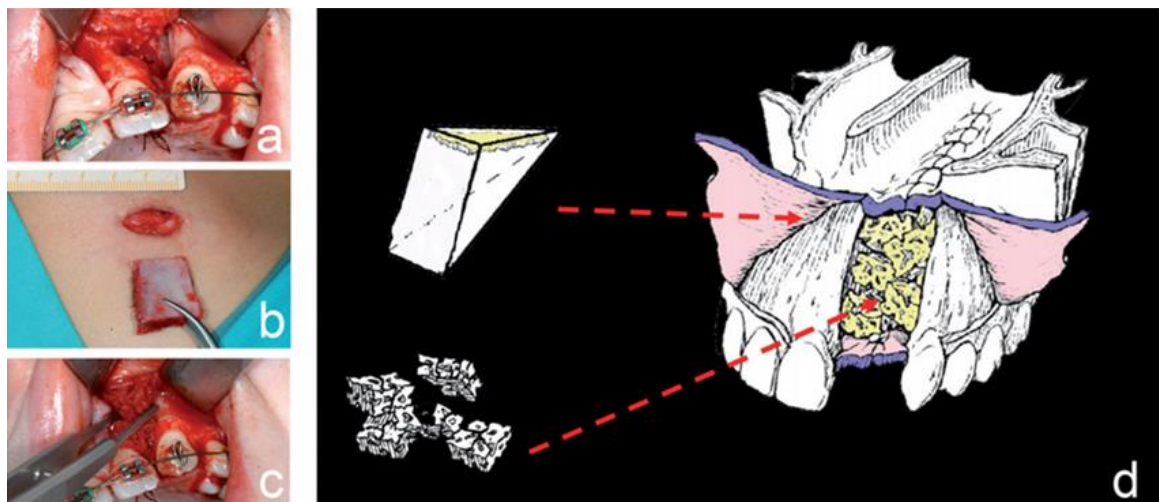
Figure 0.4.2 a) Alveolar cleft prior to placement of graft, b) harvesting of a pyramidal bone block from the iliac crest, c) packing of the cancellous bone in cleft area, d) design of the pyramidal corticocancellous graft. Luque-Martín et al. 2014.

The use of alveolar bone grafting from the iliac crest has a very high success rate with a very low incidence of complications in patients before the age of 15 (Luque-Martín et al. 2014). However, when teeth are not present to erupt through the graft, partial resorption of the graft

occurs (Cohen et al. 1993). Resorption occurs when there are no teeth to erupt, due to the lack of biological stimulation in the area of the graft. The biological stimulus favors the migration of cells and also increases blood supply.

3.5 Image Analyses Technique

Techniques for evaluating internal structures of the human body, in vivo and ex vivo, are relevant strategies to understand anatomical and morphological changes in the development of different diseases, in addition to the responses to the selected treatments over time. Computational micro-tomography (micro-CT) is a high-resolution imaging modality capable of analyzing bone microarchitecture in animals (Campbell et al. 2014). This technology has undergone sophistication in the last decades, useful in several preclinical applications (Clark and Badea 2014).

According to Campbell et al. 2014, the micro-CT presents relatively low costs and allows evaluating, in addition to bone structures, soft tissues such as adipose, vascularization processes and cartilage. Regarding bone tissue, computerized microtomography technology can be used to provide quantitative data on bone microarchitecture.

Quantitative information on bone trabeculae and their densities, as well as bone resorption and deposition processes can be obtained. As the x-ray is transmitted through the sample, relative linear layers of the studied object are represented in images as gray scale values (Wu et al. 2014).

Thus, micro-CT produces three-dimensional tomographic data with microscopic resolution (voxel size $\leq 100\ \mu m$), using several hundred projections of two-dimensional conic beams from different angles (Clark and Badea 2014). Micro-CT analyzes constitute important tools in clinical and animal experiments in order to diagnose and evaluate bone diseases, as well as the process of tissue regeneration over time.

3.6 Computed bone mapping from 3D tomography

Oh, Tae Suk et al. 2015, analyzed the risk factors for bone resorption following secondary bone grafting in the alveolar cleft, using three-dimensional (3D) computed tomography (CT) based

on surgical simulation software (SimPlant OMS, Materialise Dental, Leuven, Belgium). Each data set was measured by three different analysts and the inter- and intra-observer variability was calculated, to validate the measurements. They observed that only dental appliance and canine eruption were significantly correlated with graft survival. They conclude that measurement of an alveolar bone defect using a simulation program based on 3D CT is reliable and reproducible and also verified that secondary bone grafting survival was significantly correlated with canine eruption and dental appliance.

Nagashima et al. 2014, evaluated the initial defect and the outcome of bone grafts for unilateral alveolar cleft using computer-aided engineering (Fig. 3.6.1). They illustrated the change in bone volume using computer-aided engineering (CAE) based on multi-detector row computed tomography scan data. They evaluated 29 patients that underwent bone grafting between 8 and 14 years of age using iliac crest bone grafts, computed tomography were taken immediately preoperatively and at 1 month and 6 months postoperatively and the defects at the alveolar cleft and volume of the bone graft were determined for each patient. They concluded that this method can provide universal evaluation of alveolar bone graft volume.
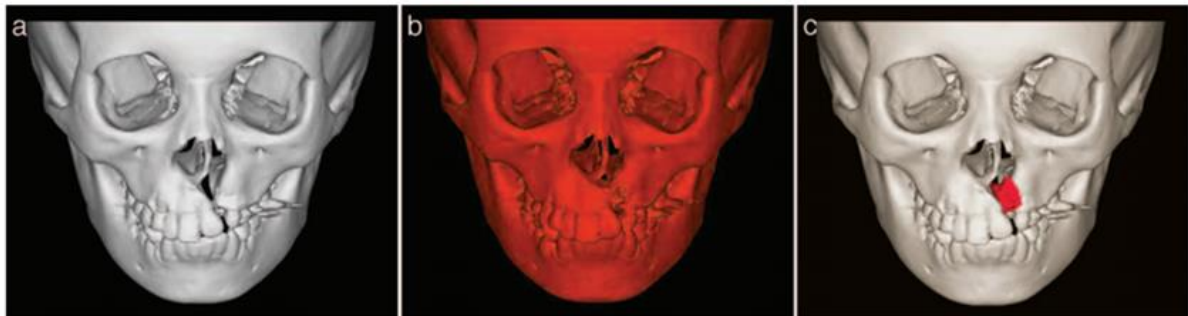
Figure 3.6.1 Evaluation method using computer-aided engineering CAE. a) Preoperative polygon model of the bone, b) Six-month postoperative polygon model of the bone, c) Overlay of the pre and postoperative images. Note that the difference is represented as bone graft volume. Nagashima et al. 2014.

Campbell. et al. 2014, analyzed the use of the micro-CT as a high-resolution imaging modality that is capable of analyzing bone structure with a voxel size on the order of 10 μm. Analyzes were discussed, and the routinely used bone architectural parameters were outlined. They created a protocol that outlines the common procedures that are currently used for sample preparation, scanning, reconstruction and analysis in micro-CT studies. They concluded that a

balance must be found between image quality and administered radiation dose to avoid affecting the parameters measured in the study.

Clark et al. 2014, reviewed several image reconstruction strategies based on interactive, statistical and gradient sparsity regularization, demonstrating that high image quality is achievable with low radiation dose given ever more powerful computational resources. They concluded that micro-CT provides a reliable platform for small animal imaging that is complementary to other small animal imaging methods, enabling numerous morphological and functional imaging applications.

3.6.1 The Hounsfield Unit scale (HU) used at the Dolphin software to analyze CBCT

The difference between CBCT and a conventional CT is that CBCT uses a cone-shaped beam that captures the full image in a single rotation. The patient should not move during the exam. Technically, it is a squared matrix of pixels (picture elements), each representing a voxel, in a slice of the region of interest. The series of measurements collected by the CT scanner are assigned a gray value based on the magnitude of contrast. Slightly attenuating structures like air are shown in black, and the highly attenuating structures like compact bone are shown in white (Fleckenstein and Tranum-Jensen 2014).

For image reveal, each pixel is appointed a CT number representing tissue density; this number was created by Sir Godfrey Hounsfield.

Hounsfield unit scale (HU) refers to the linear transformation of the original linear attenuation coefficient value of each tissue, and it measures radio density on a quantitative scale (Hounsfield 1973). HU values for CT machine was first defined as -1000 HU for air while distilled water was defined as 0 HU (Razi et al, 2014) (Fig.3.6.1.1). HU is not an absolute value and can change based on imaging parameters and CT scanners. For instance, the initial HU values were represented from -1000 to +1000 (Hounsfield 1973), while newer CT machines have a range up to 4000 HU (White and Pharoah 2014). Another important observation is that many tissues differ by only few HU, therefore only if a small range of HU is displayed those tissues can be differentiated.

In CBCT, the degree of x-ray attenuation coefficient is shown by gray scale values instead of HU scale, even though some CBCT manufacturers and software present the gray scales named as "HU". Note that this HU CBCT terminology does not hold the same value as the actual HU scale. Basically, "gray scale" and "HU" do not share the same value and scale. Still, a number of studies have observed the relationship between HU values and gray scale for bone tissue density (Katsumata et al. 2007), with generally consistent findings, although under distinct scan protocols. Nevertheless, while bone density values correlation between HU CT and CBCT gray values has been widely explored, the opposite can be said regarding literature about the correlation in values for air and soft tissue.

In CBCT, an image with low density (considered radiolucent in 2D radiographs) is called hypodense and with high density is called hyperdense. Voxels with a number below the upper limit will be displayed in black and higher than it will be in white. Due to this imaging principle, the dimensions of a structure may be distorted in regions where different tissues meet, for instance between soft tissue and bone, as the boundary may not be clearly differentiated. This distortion becomes more pronounced the thicker the sections are because more different tissue's density values will be in the same voxels (White and Pharoah 2014).
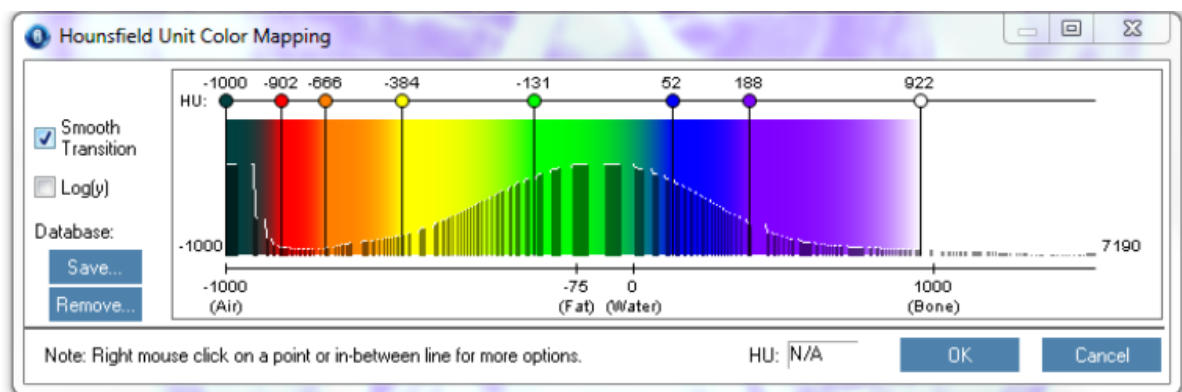
Figure 3.6.1.1 Hounsfield Unit Scale.

3.7 Hyrax Rapid Palatal Expansion

The Rapid Palatal Expansion (RPE) appliance was invented in 1860 by Angell (Angell 1860). Posterior cross-bites are usually corrected by the use of palatal expanders. The most common expanders use screws, which is Hyrax. The selection of the expansion appliance is based on the characteristics of the clinical problem as well as on the orthodontist's personal preference and experience.

Hyrax Rapid Palatal Expansion (RPE) didn't showed overall long-term different skeletal and dental changes in transverse, anterior-posterior and vertical planes. The treatment showed more expansion posteriorly than anteriorly (Davami et al. 2020).

Rapid Palatal Expansion (RPE) performed by means of Hyrax appliance followed by iliac crest bone grafting is the most common method to increase the width of the maxilla in cleft lip and palate patient. There is no bone formation in the median palatine suture in these patients, but it still promotes distancing of the maxillary segments and widening of the cleft (Long Jr et al. 2000).

Carvalho Trojan et al. 2017, showed using finite element analysis that bone stresses had peak values located in the regions where boundary conditions were applied. For just one activation of the jack screw in the expander supported by the tooth, peak stress (traction) peaks of 1.5-2 MPa were found in the alveolar bone-buccal and lingual to the supported teeth - at the beginning of the zygomatic process of the maxilla, in the nasal floor and internal walls of the nasal cavity (Fig. 3.7.1). The strain levels at the tooth-borne appliance, were lower than 2 $\mu\varepsilon$ in the anterior nasal region, between 6 and 14 $\mu\varepsilon$ in the anterior oral region, and between 8.5 and 84.5 $\mu\varepsilon$ throughout the bone surface were found, with the highest concentration in the central region between the nasal and oral floor. Based on the results obtained in this work, it was possible to improve the understanding of the stress distribution when tooth-bone expander devices were used.
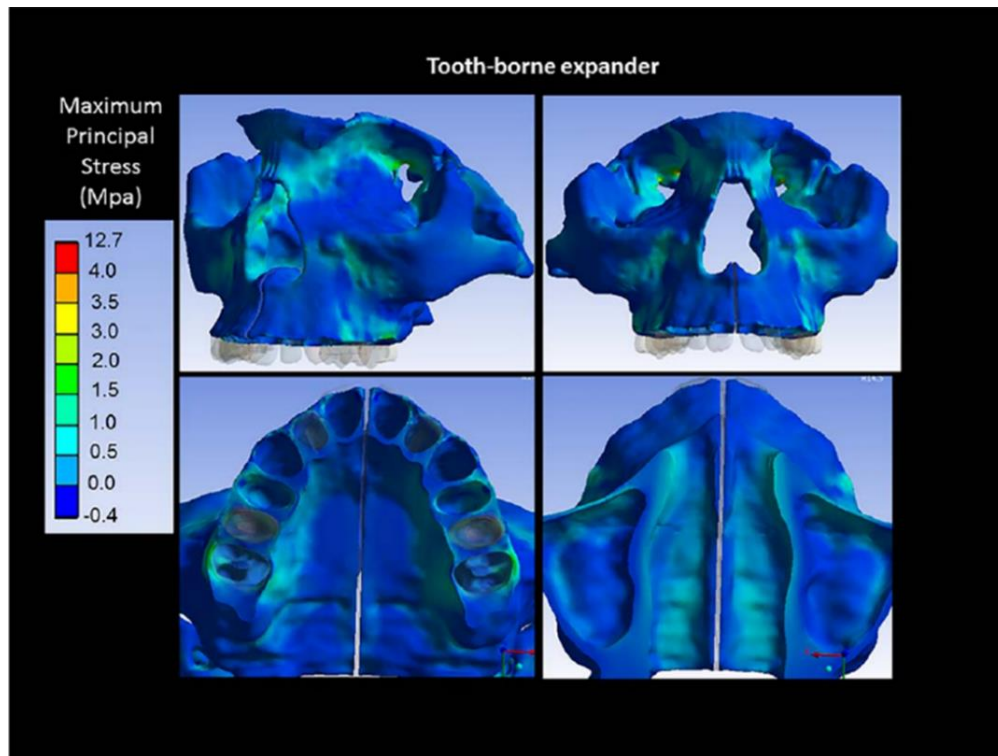
Figure 3.7.1 Distribution of maximum principal stress when displacement is applied in the tooth-borne expander (upper: lateral and frontal view; lower: occlusal view and nasal floor) (Carvalho Trojan et al. 2017).

Frost 1994, observed that mechanical fatigue damage (microdamage) normally occurs in bone. When overloading the bone, microdamage is increased and also the Basic Multicellular Unit (BMU) number and remodeling, which repair them. This can happen in fractures and in bone overloaded by endoprostheses and internal fixation implants. The predicted strain values were correlated with Wolff's Law, considering the following parameters (Table 3.7.1).

Table 3.7.1 Biological effects predicted by Wolff's Law (Frost 1994)

Strain value (με)	Biological predicted effect
< 50	Minimum effective strain range at and above which bone remodeling begins decreasing towards normal
> 1500	Lamellar bone modeling drifts turn on aiming to reduce future strain under the same mechanical loads
> 3000	Woven bone drifts on to suppress local lamellar drifts and increase bone micro damage that remodeling normally repairs
> 25 000	Bone fracture

4

CLINICAL CASE

The study was approved by the Orthodontic Clinic of the University of Minas Gerais Dentistry Faculty. The patient signs a free and informed consent form, that his data can be used for knowledge and research purposes. This study followed the ALARA principle (As Low As Reasonably Achievable) by the European Society of Radiology, thus, CBCTs were not specifically taken for this study.

The case of patient A. S. (Fig.4.1) was analyzed, he started his treatment at the Dentistry School of the Federal University of Minas Gerais, when he was 24 years old with a congenital disease and had the palate closed but the maxilla was not yet repaired, being in need for different dentistry treatments (Fig. 4.2). The proposed treatment sequence was (i) maxillary disjunction; (ii) fixed apparatus (alignment and leveling); (iii) orthognathic surgery.

Figure 4.1 The patient A. S.

Figure 4.2 The patient when he arrived at the clinic for treatment. A. The soft tissue of the palate was already closed, but the maxilla was not fixed. B. Lateral view, the maxilla is retracted because it is atresic. C. Front view, cross bite.

The hyrax appliance was installed on December 14, 2014, and the patient was instructed to activate the device with 1/4 turn for 15 days. The patient was then instructed to activate the device 1/2 turn in the morning and 2/4 turn at night for the next 10 days (Fig.4.3). During this period, the patient also underwent dental endodontics of the tooth 46.

He used the hyrax appliance to expand the maxilla and correct crossbite. After treatment with the tooth-supported Hyrax, the patient was released for bone graft surgery. This patient was submitted to the traditional treatment protocol for cleft palate bone graft surgery, used for young patients. The Hyrax device was removed to lock the screw with cold acrylic and then re-cemented so that it could be used as a retainer, a technique used by Grassia et al. 2014; Muchitsch et al. 2012.

Figure 4.3 Hyrax tooth-supported installed before the bone graft surgery.

The first CBCT before expantion with Hyrax showed the patient with unilateral cleft palate and a 6.64 mm defect to close in the maxilla, (Fig.4.4).

Figure 4.4 CBCT before treatment, 6.64mm maxilla defect.

The bone graft surgery was performed on August, 8, 2017. The pre-surgical CBCT was taken on June, 23, 2017 and, after the surgery, one CBCT was taken fifteen days later and another after sixty days.

The objective to follow-up the clinical case was to evaluate and measure the resorption of the bone graft in the patient who had the traditional treatment, used in patients under 15 years old, even he was an adult, physically mature patient, with lack of physiological stress. This case would be a reference for this study, to simulate in biomechanical models the behavior of the graft under stress, using the Hyrax appliance after the surgery.

5

METHODOLOGY

Due to the importance of studying the mechanical and biological characteristics of the newly formed bone, the aim of this study is to evaluate the maxillary bone graft in patients with cleft palate who missed the ideal time to perform it. The best period for graft implantation is between 9 and 12 years of age, when the canine eruption has not yet occurred, which favors graft success due to physiological stresses at the graft site caused by the eruption of canine and maxillary growth (Bergrand et al. al. 1986).

What is observed in late grafts in patients who have lost their best age is that most of the bone graft is reabsorbed by the body, as there are not physiological forces acting at the graft site, signaling to the body that the grafted bone is not necessary (Erica et al., 2017).

Although it is not the best moment to perform a bone graft, in an adult patient, is still essential to fix the maxilla, in this way, teeth can take their proper place and perform their functions, thus completing the patient's treatment procedure (Feichtinger et al. 2006).

In order to improve the success of late graft surgeries, it was evaluated if the imposition of tensions in the graft area, using orthodontic appliance, simulating the physiological stresses, can prevent the bone graft resorption.

To achieve the objectives of this study, the following steps will be taken:

- Evaluation of a patient CBCTs, who underwent bone graft surgery after the appropriate age, following the evolution of the graft for 2 months. The CBCTs were performed, one before surgery, and another two, with 15 and 60 days after surgery;
- A maxillary bone failure associated with bone graft surgery was performed in mice to collect data of the bone evolution remodeling and how the "grounded bone" placed at

the graft area became neoformed alveolar bone. The quality of the microarchitecture of the bone and its density were measured.

- 3D models were created from the patient CBCT to simulation of the stresses that can stimulate the maintenance of the graft in the maxilla, to promote its fixation;

- Finite Element Analysis (FEA) were used to investigate the distribution of internal stresses. Simulations were performed in the ANSYS Workbench to mesh the geometry and analyze the stress distribution in patients with cleft palate.

5.1 CBCTs of the patient

Comparisons of cone beam computed tomography (CBCTs) images were performed to evaluate the evolution of the bone grafted tissues. The CBCTs scans of the patient were evaluated; the patient had a preoperative CBCT scan (Fig.5.1.1) and other two CBCTs with 15 (Fig. 5.1.2) and 60 days after surgery.

The CBCT scans were acquired with the I-CAT 3D Dental Imaging System, using a standardized protocol (large field of view (FOV) 8cm x 8 cm, voxel size 0.2mm, 120 kVp, 36,12 mAS, 40 seconds). Vertical laser beam (at midsagittal plane) and horizontal beam (at Frankfort horizontal plane) were used to orient the patients' heads. The CBCT data was exported as DICOM files (Digital Imaging and Communications in Medicine).
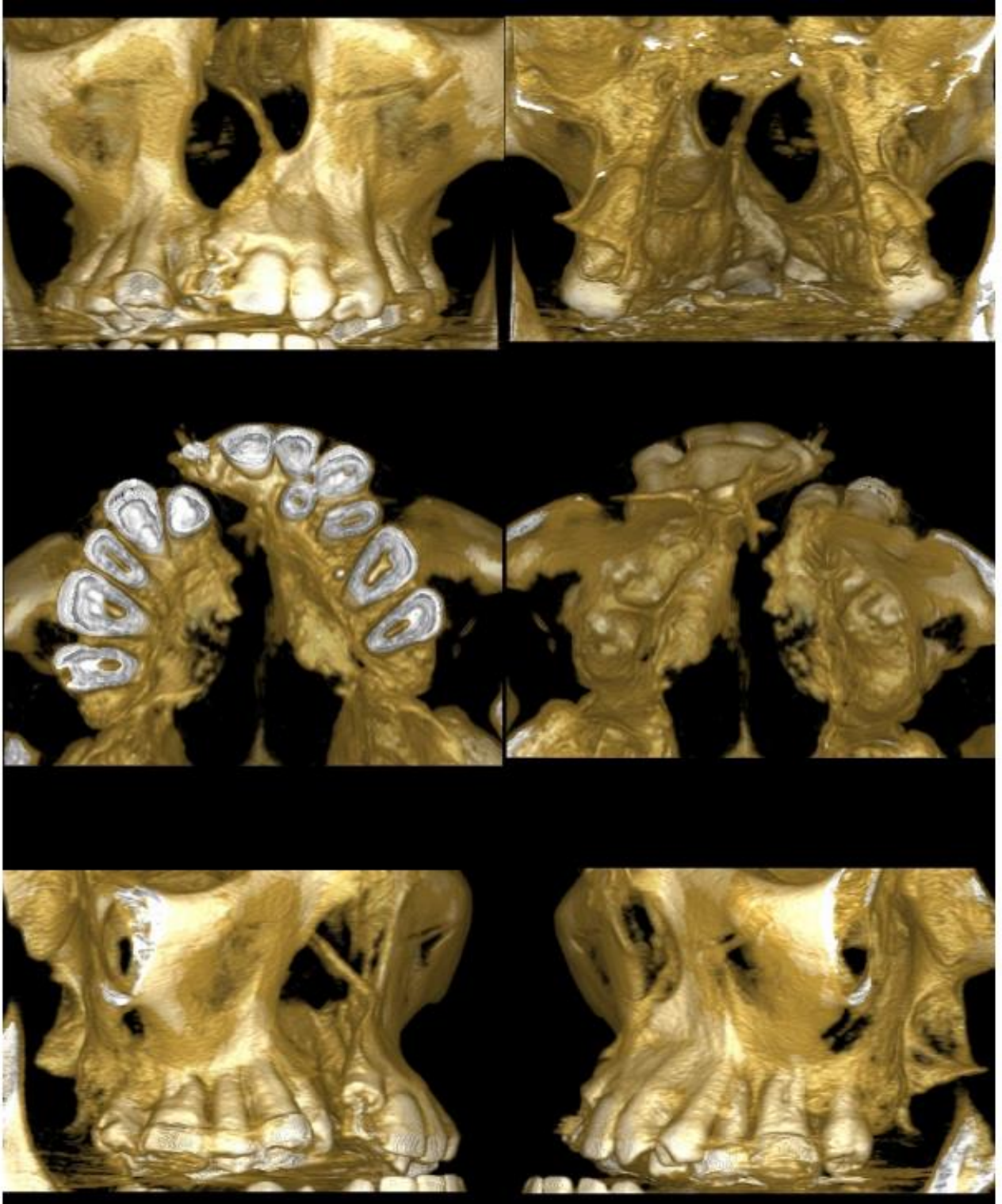
Figure 5.1.1 Patient's tomography before secondary bone graft surgery.
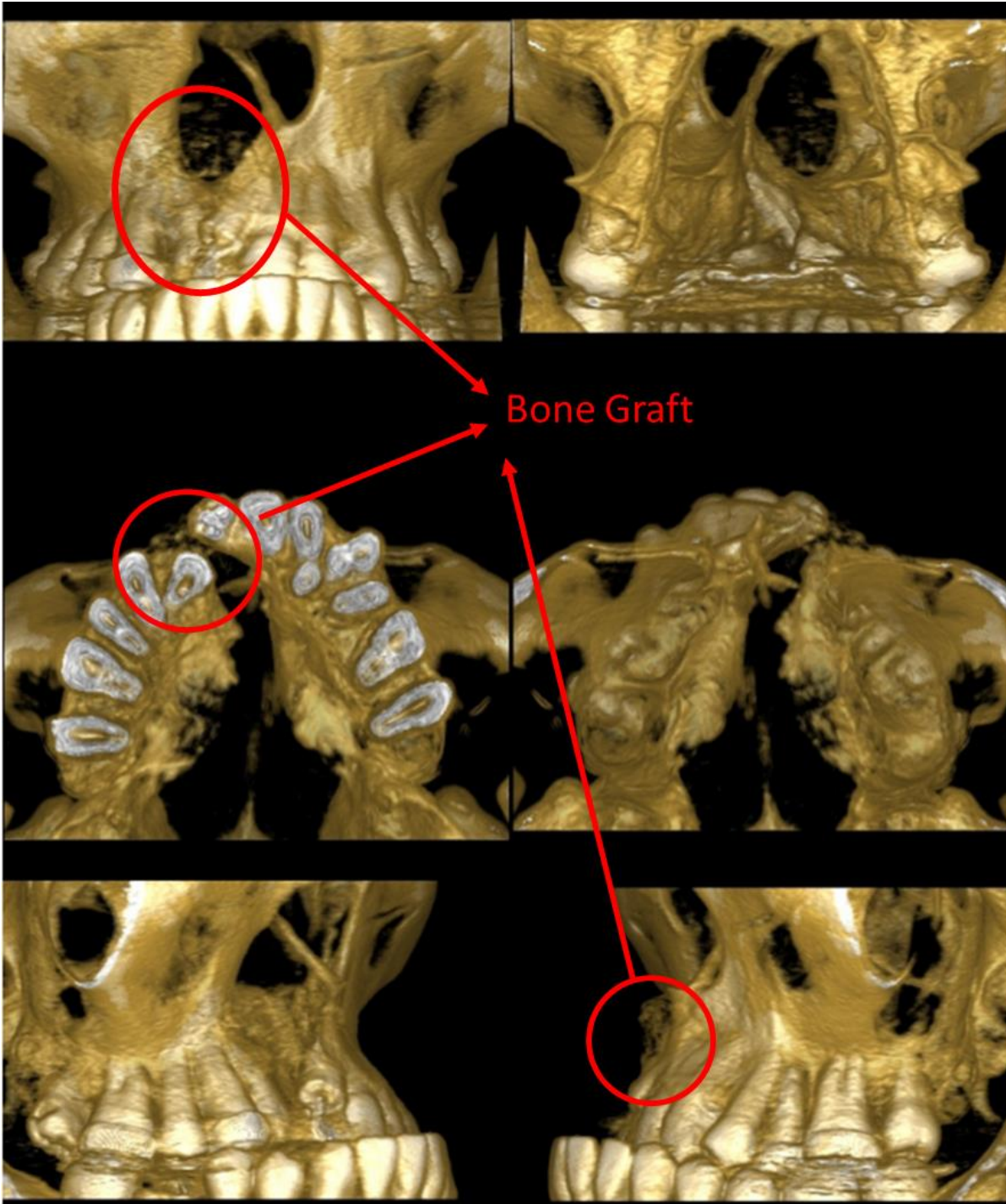
Figure 5.1.2 Patient's tomography 15 days after late secondary bone graft surgery.

5.2 Evaluation of the volume and density of the bone graft

The CBCT data was exported as DICOM files (Digital Imaging and Communications in Medicine) and loaded into automated reconstruction commercial software Dolphin 3D (version 11.95 premium, Dolphin Imaging & Management Solutions, Chatsworth, CA, USA), to obtain the volume of the bone graft, the methodology was previously described by Thereza-Bussolaro et al. 2020 and was adapted for bone measurement.

First the orientation of the skull was fixed in order to standardize the assessments. The skull was oriented in frontal view at the midsagittal plane by the nasal septum (vomer). In the right view, the coronal planes were oriented by the most anterior portion of the alveolar bone and the axial plane was oriented by the mandibular notch (Fig.2).
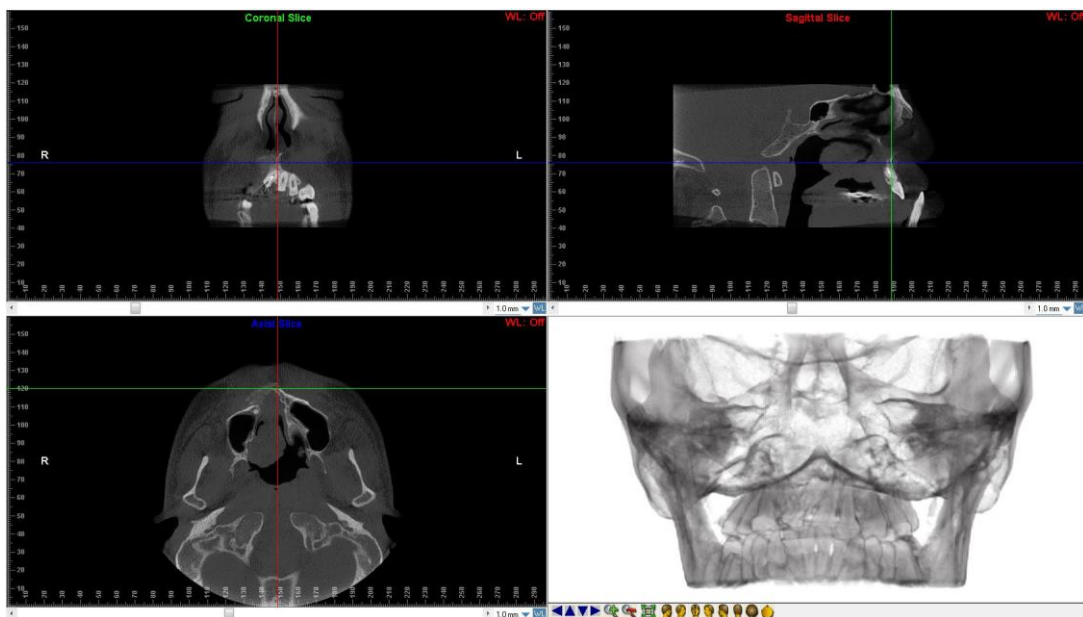
Figure 5.2.1. Reliability and HU values collection

Two observers (E.T., and C.T.B) defined 6 landmarks (in each scan timeline) to verify Dolphin HU's values of the graft and the region to serve as control. The density of the graft was assessed by means of these Dolphin HU's values. In axial view, three landmarks were chosen in the graft (Fig. 4.2.2 A), and three for the control region (Fig. 5.2.2 B). Those landmarks were carefully scanned (scrolled) 5 times for each observer and the lower and the upper Dolphin HU's values were collected.

The density data varies from software to software and from CBCT to CBCT. Due to this, firstly, it was necessary to compare the density of the graft with a known density in the same CBCT. This was achieved by observing the density of the trabecular bone in another location of the maxilla (Fig. 5.2.2 B), here called control region. These reference points were carefully scanned (scrolled) five times for each observer. The values of each point's lower and upper density were collected, thus determining the limit to be used to obtain the volume.
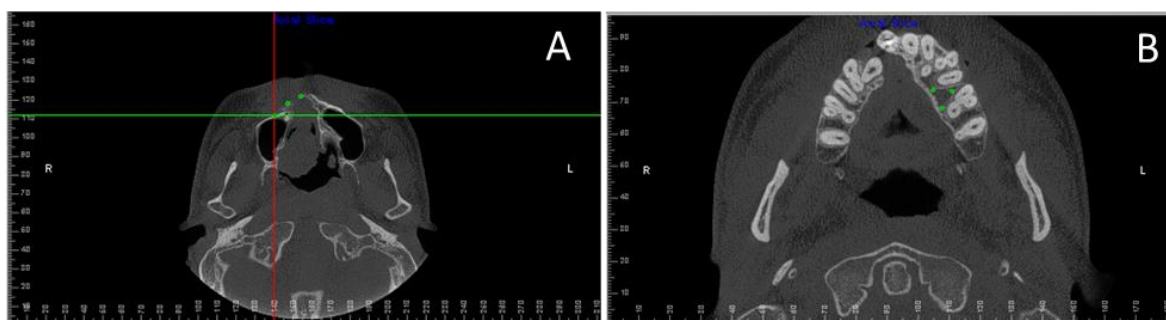
Figure 5.2.2 A) In axial view 3 landmarks were chosen in the graft; B) 3 landmarks were chosen for the control region.

For bone volume rendering, a previously reported technique was adapted (Thereza-Bussolaro 2020). Manual segmentation and contouring around the graft (green dots) were performed in axial and sagittal view (Fig. 5.2.3 A and B). After the delimitation, seeds points (yellow dots) were placed, and the inverted threshold tool were selected for the bone graft region (Thereza-Bussolaro et al. 2020), using the threshold defined by the lower and upper density values previously found. Next, the volume was automatically calculated and rendered by the software.
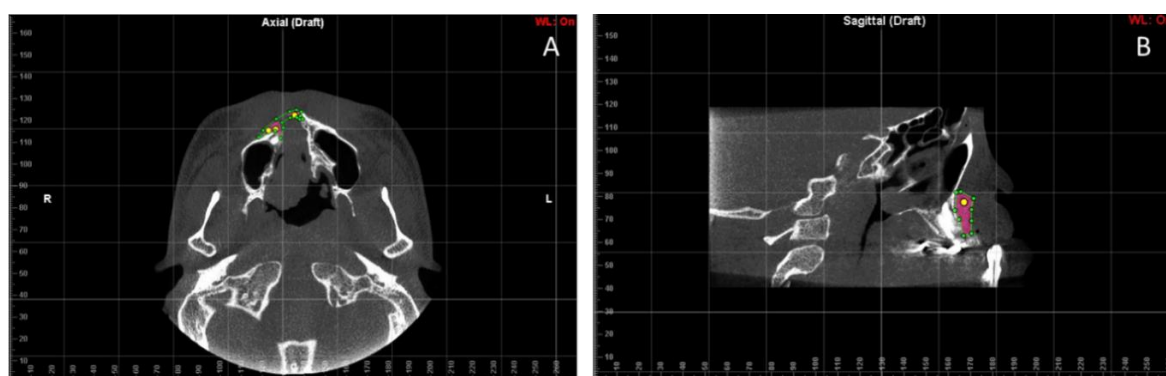
Figure 5.2.3 A) Contouring around the graft (green dots) were performed in axial and B) sagittal view. After the delimitation, seeds points (yellow dots) were placed.

For the control region, the same three landmarks were also used to render the volume. A triangle was built with the base in palatal bone. The same process of inverted threshold and density previous found for the control were used to define the threshold limit (Fig. 5.2.4 A and 5.2.4 B).

Figure 5.2.4 The control volume region, sagittal view (A) and lateral view (B).

Finally, the volume for the control region was also automatically calculated and rendered by the software (Fig.5.2.5 A and B).
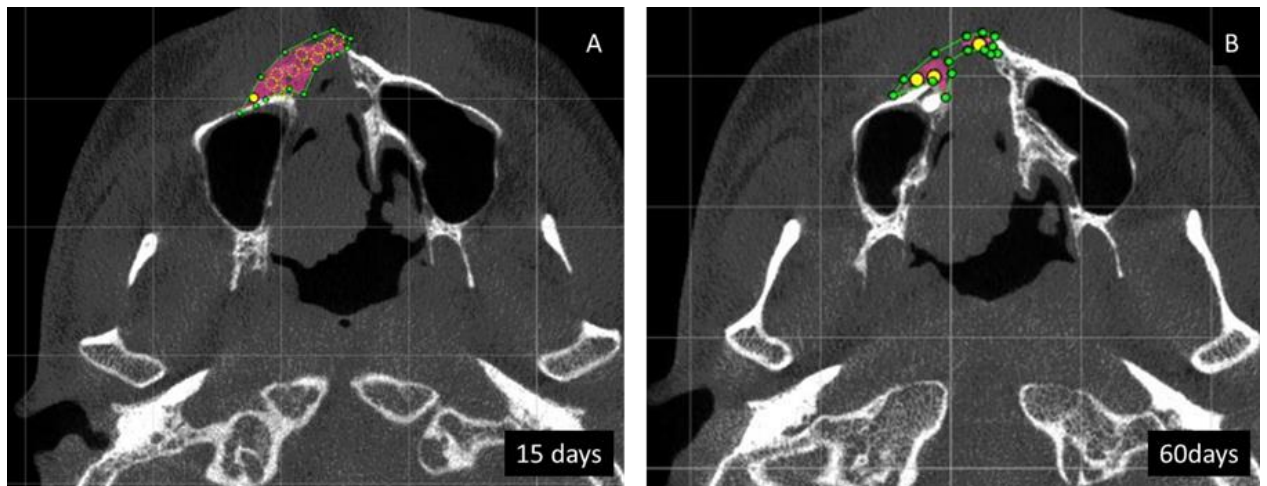
Figure 5.2.5 A) Volume calculation with 15 days and B) 60 days.

Dolphin describes the difference in tissue radiodensity by different colors. Figure 5.2.6 shows the CBCT scans at different times analyzed in this work. It is possible to observe the variation in the volume of the bone graft during the post-surgical process.
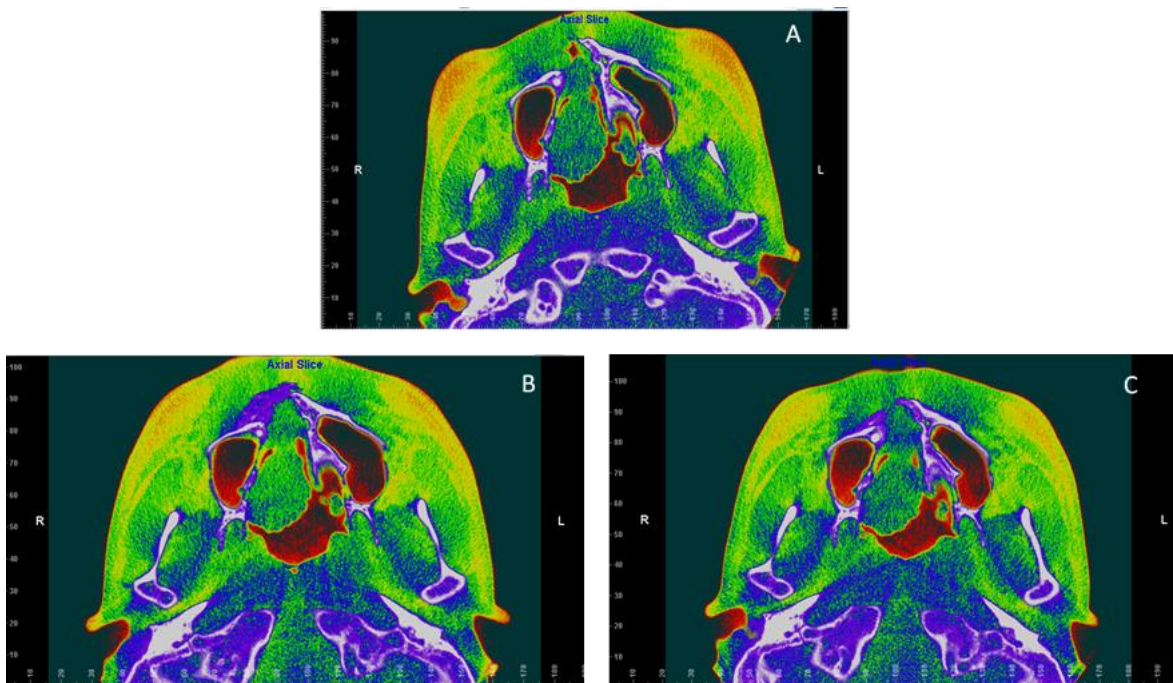
Figure 5.2.6 A) CBCT HU's variation before bone graft. B) After the surgery, two CBCTs were taken with 15 days and C) 60 days to analyze the volume and the density of the bone graft.

The volume was automatically calculated and rendered by the software as shown in Figure 5.2.7A. The bone graft with 15 days after the surgery had a volume of 1123 mm³ and 5.2.7B, 60 days after the surgery with the volume of 365mm³.
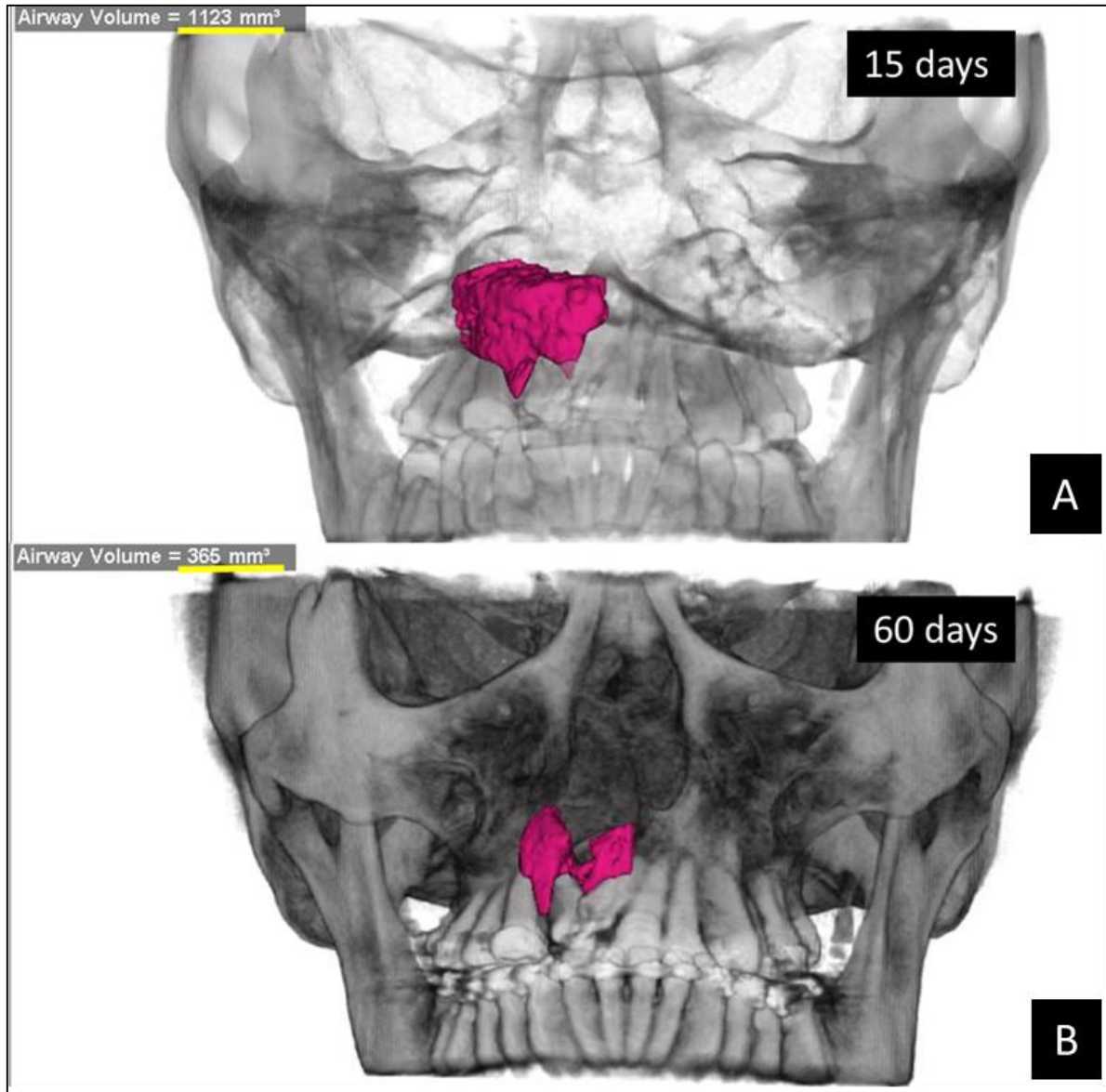
Figure 5.2.7 A) Bone graft with15days after the surgery and B) Bone graft with 60 days after the surgery.

Statistical Package for the Social Science (SPSS, IBM, version 26; SPSS Inc., Armonk, NY, USA) was used to assess intra and inter-reliability of both observers (ET and CTB) through Intra-class correlation coefficient (ICC) test, and to analyze de differences in bone graft volume and density between the two bone graft's time points (T1 and T2) through T-Test. The level of significance and confidence interval (CI) was set at 0.05.

5.3 Animal experimental model analysis

5.3.1- Evaluation of the bone graft evolution to neoformed bone tissue

In this experiment we had bone donor animals and experimental animals. The femur of donor mice was removed and ground for bone graft purpose, while the experimental mice were submitted to bone defects created on the right and left sides of the alveolar bone using a diamond spherical drill number 8, in order to simulate the maxillary defect, present in patients with cleft lip and palate. The left side was grafted while the right side was the negative control, with no graft treatment.

Twenty-five C57 BL6 male mice were used, and divided into the following experimental groups (Table 5.3.1):

Table 5.3.1 Animals groups

	Number of animals (n)	Time for euthanasia after surgery
B	1	0 hours
D1	4	24 hours
D7	5	7 days
D14	5	14 days
D21	5	21 days
C	5	21 days

Experimental B (bone donor). Bone donor animal: an animal donor was euthanized by anesthetic overdose (ketamine 300 mg/kg + xylazine 30 mg/kg) followed by cervical dislocation on the same day of the experiment from each subsequent described group. After euthanasia, the femur was removed, macerated ("ground bone" formation) and used as a bone graft in the region of the bone defect caused in the experimental animals.

Experimental D1: after anesthesia (ketamine 100 mg/kg + xylazine 10 mg/kg) two bone defects were created in the right (R) and left (L) sides of the alveolar bone of the mice using the diamond drill. The left side was filled with macerated bone and the right side was used as a negative control. The animals were euthanized 24 hours after the surgery. The left side of the jaw was used as the control.

Experimental D7: after anesthesia (ketamine 100 mg/kg + xylazine 10 mg/kg) the bone defect were created using the diamond drill on the palate of the mice and two bone defects were created in each animal, one was filled with macerated bone and the other wasn't. The "ground bone" was placed on the left side of the donor animal, thus simulating the lip-palatal fissure and the placement of the bone graft. The animals were euthanized 7 days after the surgery. The left side of the jaw was used as the control.

Experimental D14: after anesthesia (ketamine 100 mg/kg + xylazine 10 mg/kg) the bone defect were created using the diamond drill on the palate of the mice and two bone defects were created in each animal, one was filled with macerated bone and the other not. The "ground bone" was placed on the left side of the donor animal, thus simulating the lip-palatal fissure and the placement of the bone graft. The animals were euthanized 14 days after the surgery. The left side of the jaw was used as the control.

Experimental D21: after anesthesia (ketamine 100 mg/kg + xylazine 10 mg/kg) the bone defect were created using the diamond drill on the palate of the mice and two bone defects were created in each animal, one was filled with macerated bone and the other not. The "ground bone" was placed on the left side of the donor animal, thus simulating the lip-palatal fissure and the placement of the bone graft. The animals were euthanized 21 days after the surgery. The left side of the jaw was used as the control.

Experimental C (Control): After anesthesia (ketamine 300 mg/kg + xylazine 30 mg / kg), the animals were euthanized without any surgical intervention. The animals were euthanized, at the same day as the last group, 21 days after the surgery.

After euthanasia the maxilla were collected for:

(1) Analysis of the bone microarchitecture and density by micro CT;
(2) Histomorphometric analysis with hematoxylin and eosin (HE) staining to measure the shape or form of the bone tissue and provides information about the amount of bone and its cellular activity.

5.3.2 Bone defect and bone disease surgery

Bone donor animals were euthanized by anesthetic overdose (ketamine 300 mg/kg + xylazine 30 mg/kg) followed by cervical displacement on the same day of each experimental group. After euthanasia, the femur was removed, macerated (formation of the "bone powder") using sterile grade and pistil and used as a bone graft in the region of the bone defect caused in the experimental animals.

After anesthesia (ketamine 100 mg/kg + xylazine 10 mg/kg), the animals receiving the bone graft had the palate prepared with two holes, made with a spherical number 8 drill (Fig.5.2.3.1-A). The "ground bone" was placed on the left side of the donor animal (Fig.5.3.2.1-B), thus simulating the lip-palate cleft; the right side of the maxilla was used as control. This technique was based on articles by Nguyenet al. (2009) and Kim et al. (2013), who introduced a bone defect in the rat maxilla for analysis of alveolar bone regeneration. However, as our experimental animal model were mice, it was necessary to make modifications of the technique to make the experiment viable. The animals were fed with softened feed with filtered water after the surgery.

Due to the small extension of the bone defect area, the femur of a single donor animal was used for bone grafting of approximately 20 receptors animals.
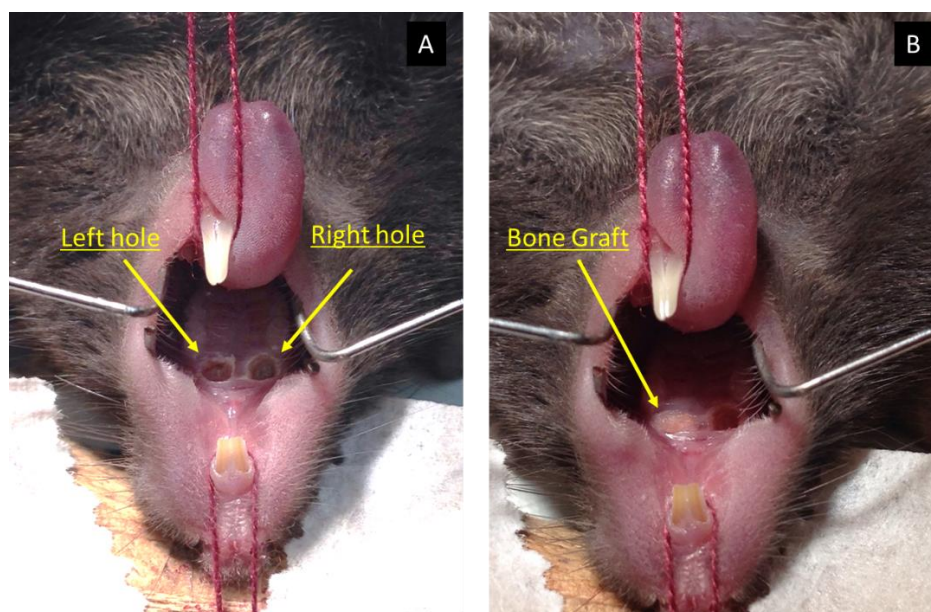
Figure 5.3.2.1 Surgery of the mice; A) Palatal holes to simulate the palatal fissure, B) Bone graft with the grounded bone from the femur on the left side

5.3.3 Animals micro-computed tomography

The maxilla collected after the euthanasia was used to assess the trabecular bone morphology using a high-resolution micro-computed tomography (mCT) (Fig.5.3.3.1).
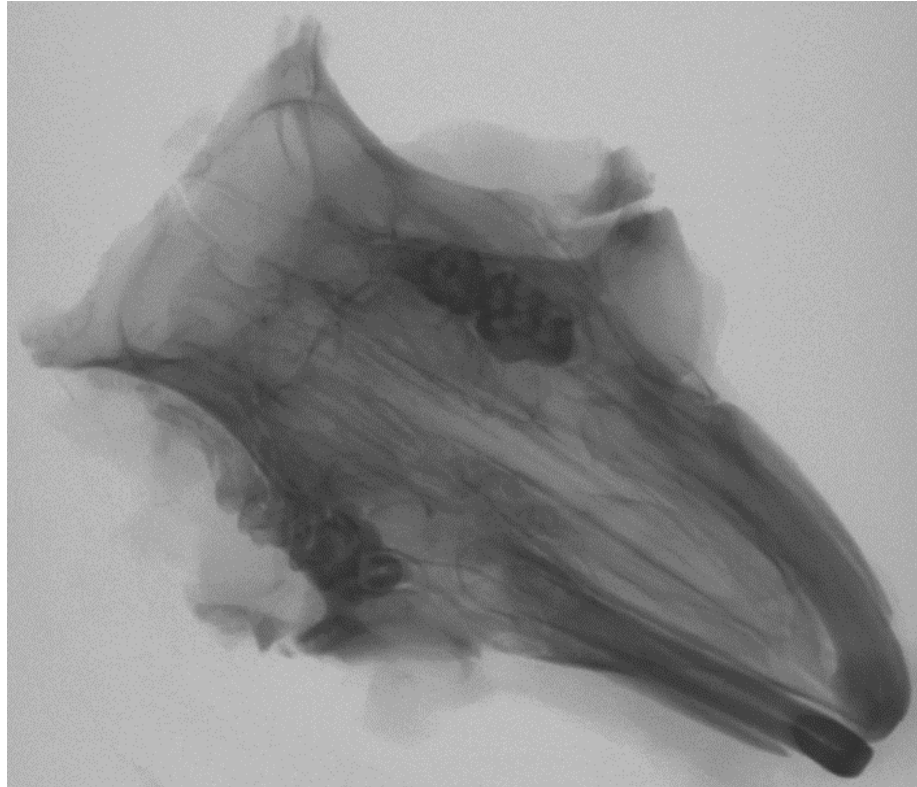
Figure 5.3.3.1 Micro Computed Tomography of the mice maxilla.

The basic morphometric indices to measure the 3D micro-computed tomography are bone volume (BV) and total volume of interest (TV). These indices can be derived from either a simple voxel-counting method or a more advanced volume-rendering method, also referred to as volumetric marching cubes (VOMACs) (Müller and Rüegsegger 1995). The ratio of these two measurements is named bone volume fraction (BV/TV). Another basic measurement is the bone surface (BS). Dividing respectively the total volume or bone volume, one can have the surface density (BS/TV) and specific bone surface (BS/BV), (Bouxsein et al. 2010).

Based on 3D calculations, a sphere fit method, the sphere thickness measurements are fitted to the object. With this method, it is possible to access the reasonable average thickness of the structure or bottom, where this reflects the average trabecular separation. For measurement of separation, the spheres are set to the bottom, where (Tb.Th) means trabecular thickness, (Tb.Sp)

means trabecular separation, and (Tb.N) means trabecular number. The sphere fit method is used to determine the diameter of the largest possible sphere that can be fitted across each voxel that is completely contained in the object (or bottom) and then to average those diameters.

The average trabecular number is calculated as the inverse of the average distance between the middle axes of the structure, using the distance transformation method. (Danielsson 1980). An advantage of this approach to computing trabecular morphometry, is that not only mean values, but also the variation of those measures, are calculated and expressed by the standard deviation. (Hildebrand and Rüegsegger 1997) (Fig.5.3.3.2).
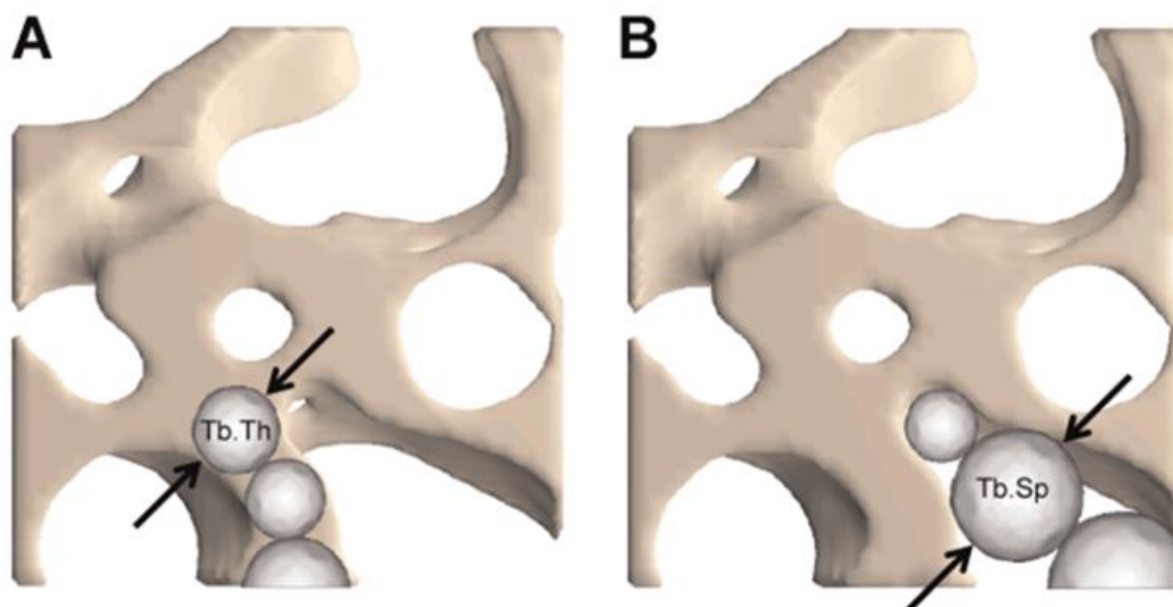
Figure 5.3.3.2 Schematic representation of algorithms used for direct 3D method for calculating trabecular thickness (A) and separation (B). (Image courtesy of Andres Laib, PhD, Scanco Medical AG). (Bouxsein et al. 2010).

5.3.4 Histomorphometric analysis

The maxillary bones were fixed for 20 days in 10% formaldehyde, decalcified in 14% EDTA solution (pH 7.4). The solution was changed daily and the bones were washed for 4 hours in running water. The maxilla was then cut using a razor into 2 sagittal sections. The skeletal fragments containing the upper three molars and alveolar bone with and without graft were

analyzed. Once the histological processing of the fragments was done, the same samples were immersed in paraffin.

The skeletal fragments were then sectioned into 4µm slices and stained with hematoxylin and eosin. Histological observation was performed using a universal microscope (Leica DMRE with a camera Leica MC170 HD (Leica Microsystems, Wetzlar, Germany) and the area of the surgery were photographed at 10 x magnification (Fig. 5.3.4.1).
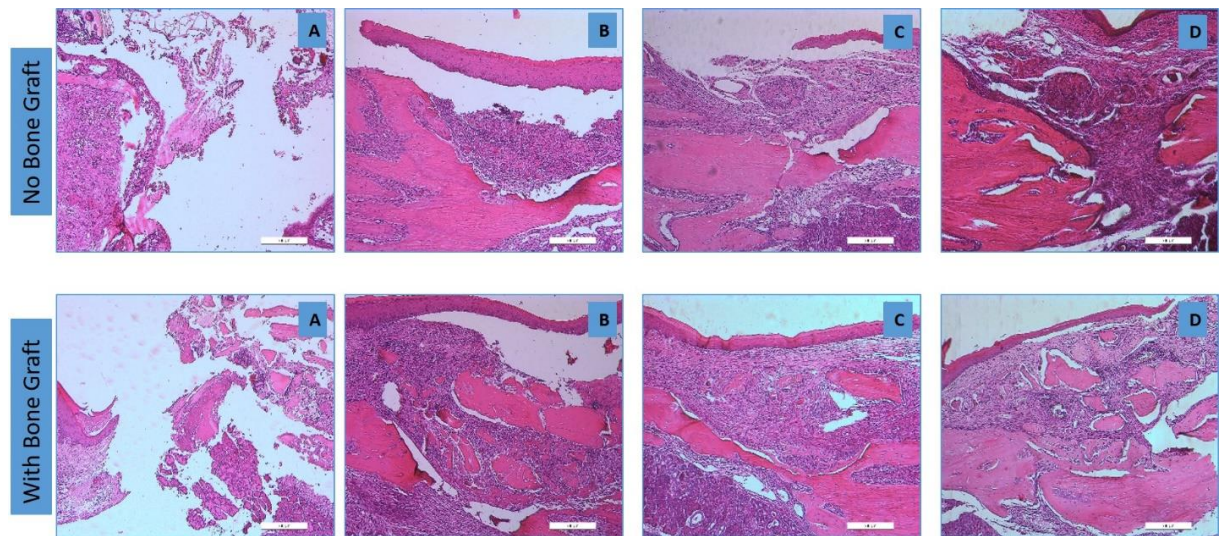
Figure 5.3.4.1 – The animals with both sides, no bone graft and with bone graft, were divided in four groups with 24 hours (A), 7 days (B), 14 days (C) and 21 days (D) after the surgery.

5.4 Finite element analysis

5.4.1 Geometric and Discrete Models

Clinical analyzes were performed by superimposing CBTCs scans obtained using the cone beam technology to identify bone formation. For the analysis by means of computational methods, a three-dimensional geometric model of the maxilla and the supporting structures of a young individual was developed.

The 3D computer model based on the CBCTs images included the palate bone with the graft area and all the teeth of the upper arch. The images were processed to generate geometric

models of the maxilla and its supporting structures to later obtain a geometric model, which was then be imported for processing in a Finite Element Analysis (FEA) commercial software.

The mechanical characteristics of the bone graft were used to reproduce clinical conditions. The constitutive model used for the consolidating bone was developed in a project with the Universidad Nacional in Bogota to account for the mechanobiological behavior for this tissue.

The flow chart of the steps of the FEM analysis are listed in Fig. 5.4.1.1. The software used in every step are also named in the colored boxes.
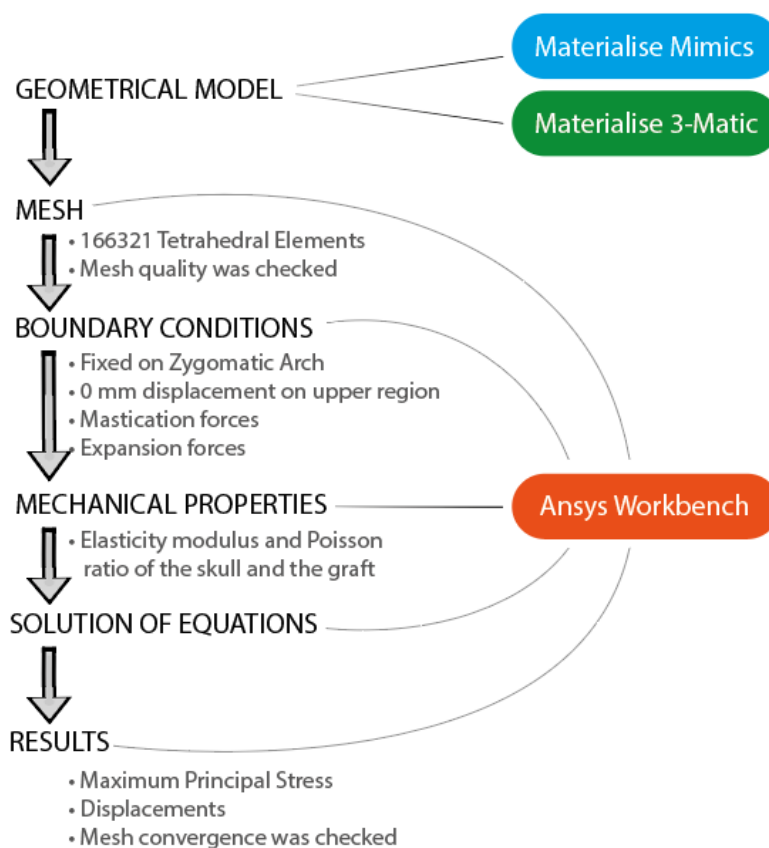
Figure 5.4.1.1 - Flowchart of the FEM analysis.

A better understanding of the stress distribution during orthodontic movement after the secondary graft as well as the biomechanical analysis of the response as a function of the bone graft evolution in these patients can be obtained. (Dewinter et al., 2003, Peamkaroonrath et al., 2011, Erica et al., 2017). An extension of the analysis for other patients can then be done after validation of the simulation with the proposed model.

Images generated by a scanner in DICOM format were processed in the 3D image processing and model generation software Simpleware® (Innovation Center, Exerter, UK, 2009). The software allows to distinguish between various tissues on the images using the contrast (radio opacity) as a criterion. The main components of the model were the alveolar bone, dental elements and periodontal ligament.

The geometrical model obtained in Simpleware® was be exported to CAD software Rhinoceros (Robert McNeel& Associates) to smoothen and transform the model elements into NURBS surfaces, which are distinguishable as individual parts of the model in FEM software (Fig. 5.4.1.2 and 5.4.1.3). The finite element analysis was performed using Abaqus/CAE® 6.13.

A validation based on the clinical follow-up of selected patient was used to validate the obtained numerical analysis. Numerical simulations were then performed to establish the best time for maxillary expansion in adult patients with cleft palate.
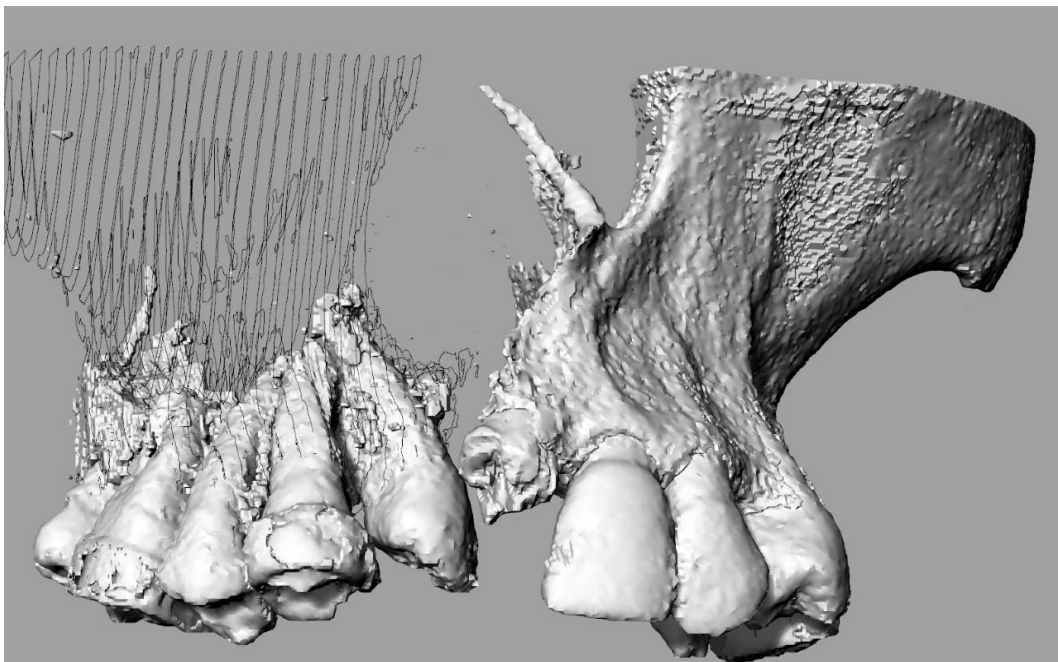
Figure 5.4.1.2 Software Rhinoceros (Robert McNeel& Associates) to smoothen and transform the model elements into NURBS surfaces. A frontal view.
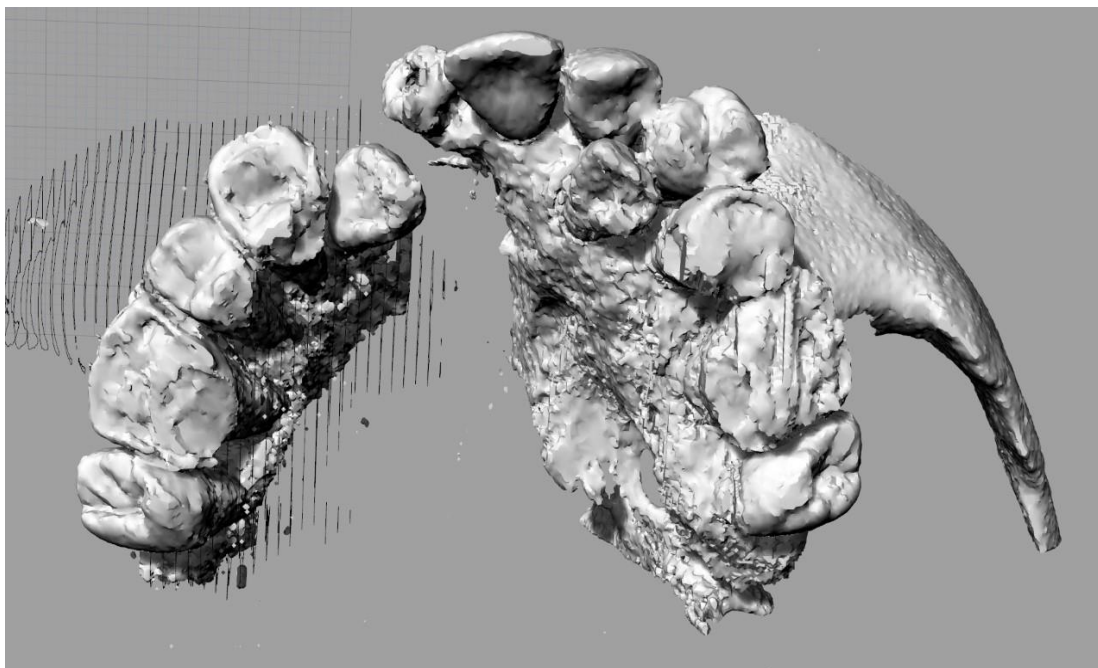
Figure 5.4.1.3 Software Rhinoceros (Robert McNeel& Associates) to smoothen and transform the model elements into NURBS surfaces. A bottom view.

Initially, the DICOM files (.dcm) from patient's 15 and 60 days' tomography were loaded on Mimics Research for 64-bits (version 17.0.0.435). One 3D model was generated for each tomography, creating a Mimics Documents file (.mcs).

The models were visually and anatomically improved. The quantity of imperfections limited what could be done, because it was difficult to separate the anatomy from the errors on the image.

The main goal was to create a model for the bone graft. The 15-day tomography was used to generate the 3D image; however, it was an approximation (Fig. 5.4.1.4 and 5.4.1.5).
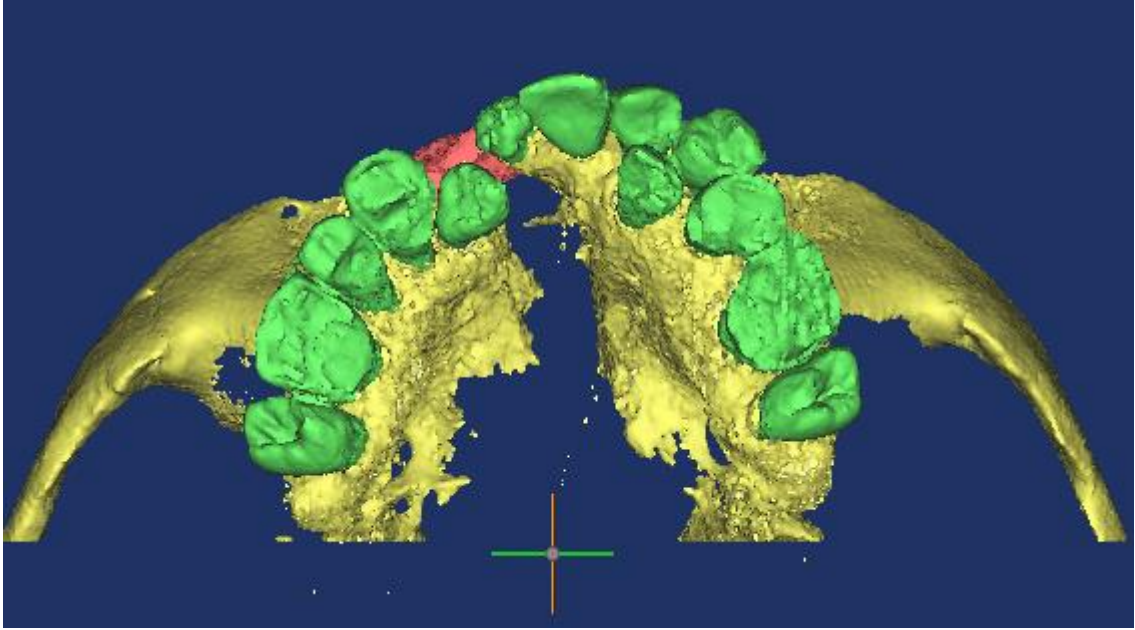
Figure 5.4.1.4 Bottom view of the bone graft after 15 days of the surgery model.
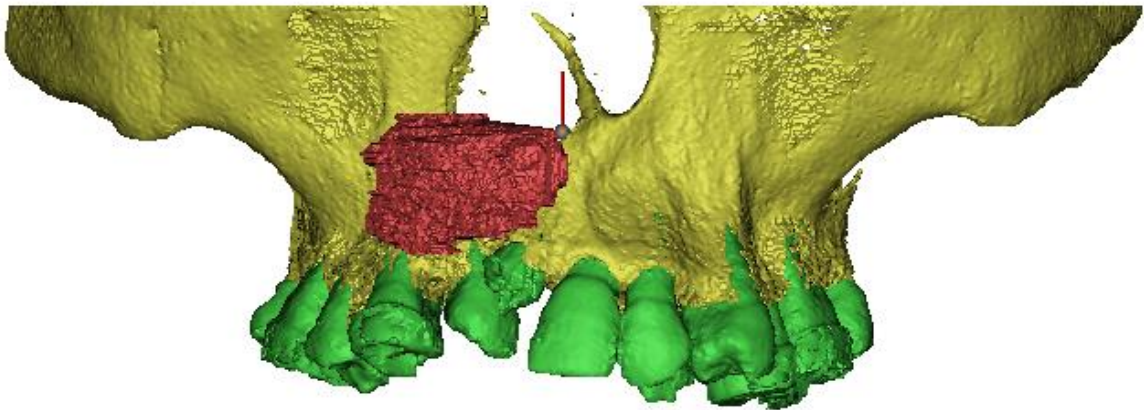
Figure 5.4.1.5 Front view of the bone graft after 15 days of the surgery model.

The graft was separated (red area on the image above) from the rest of the model, exported to a STL file and imported on Abaqus. Through Abaqus, a finite element simulation was done to analyze the effect of the force stimulation on the bone formation process.

5.5 Biomechanical Behavior of a bone graft under maxillary expansion

Using the CBCT of the patient A.S., the cleft palate clinical case, the geometry was reconstructed using MIMICS 20.0 (Materialise NV, Leuven, Belgium). The CBCT used was taken after the use of the Hyrax to expansion of the maxilla. The CBCT scans were acquired

with the I-CAT 3D Dental Imaging System, using a standardized protocol (large field of view (FOV) 8cm x 8 cm, voxel size 0.2mm, 120 kVp, 36,12 mAS, 40 seconds).

A representative model of a non-cleft skull (healthy skull), was obtained from a computerized tomography image (Carestream Health/CS 9300) available in the research group's repository (GNUM Group - Group of Modeling and Numerical Methods in Engineering. Universidad Nacional de Colombia, Bogotá). The model originated from an 11-year-old female skull.

The geometry of the maxilla and frontal part of the skull was obtained after manual editing. The cleft width at the midpoints(M'-M) was 12 + 2mm, it is considered as a medium cleft (Fig. 5.5.1).
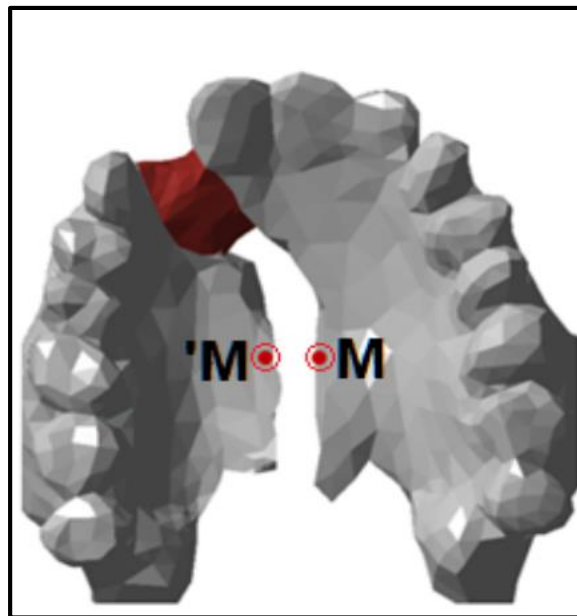
Figure 5.5.1 Points M'-M are the palatal midpoints were width was measured.

The program used to mesh the geometry into 166321 tetrahedral elements was ANSYS Workbench. Mesh quality was checked, and convergence was achieved with a change of 2.67% in the maximum principal stress (MPS) results. The line, called zone 1 (Figure 5.5.2), was chosen to evaluate points within the graft. Zone 1 also allows a comparison between the graft and healthy areas of the maxilla.
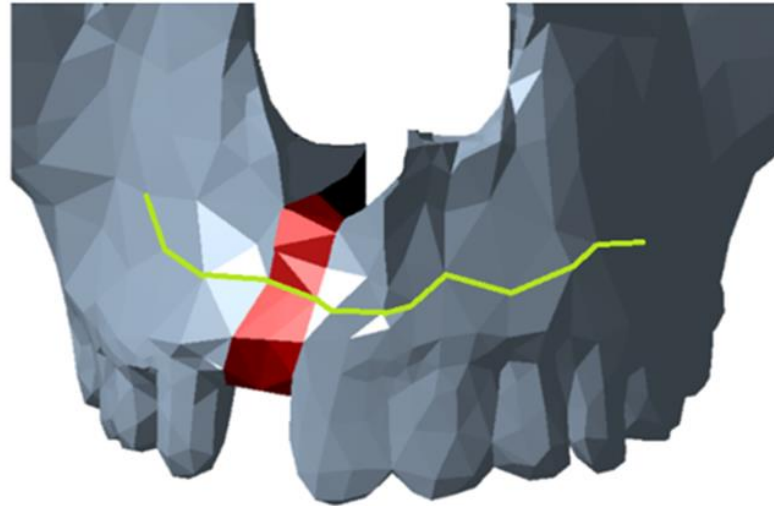
Figure 5.5.2 Zone 1 the green line shows where results of Maximum principal, shear and hydrostatic stresses were evaluated. This line includes zones within the graft (red) and healthy zones of the maxilla (grey).

5.5.1 Therapy boundary conditions

To represent the clinical situation, displacements of 0.125 mm were imposed at the palatal face of the first molars, and premolars were established, according to the displacement-controlled hyrax appliance (device responsible for conducting the expansion), which is anchored to the teeth and activated by means of a screw. A full rotation of the screw is commonly equivalent to an expansion of 0.25 mm, and typically patients will be instructed to activate the appliance in quarter rotations. Thus, 0.125 mm displacement condition was applied to the model. Static forces of 70 N were applied to both sides on the occlusal surface of the posterior teeth to simulate the forces of mastication.

As the study did not intend to investigate fatigue in craniofacial structures, cyclic chewing was disregarded. As in Trojan 2013, an intermediate value between masticatory forces of greater and lesser magnitude found in the literature (12N - 150N), then 70 N was selected.

The real model was fixed at the most posterior part, and displacements of 0 mm were imposed at the upper region as show at the Figure 5.5.1.1, where purple areas indicate fixed areas. Red and yellow arrows designate forces and displacements, respectively. Yellow areas at the RC model show the 0mm displacement condition in vertical direction.
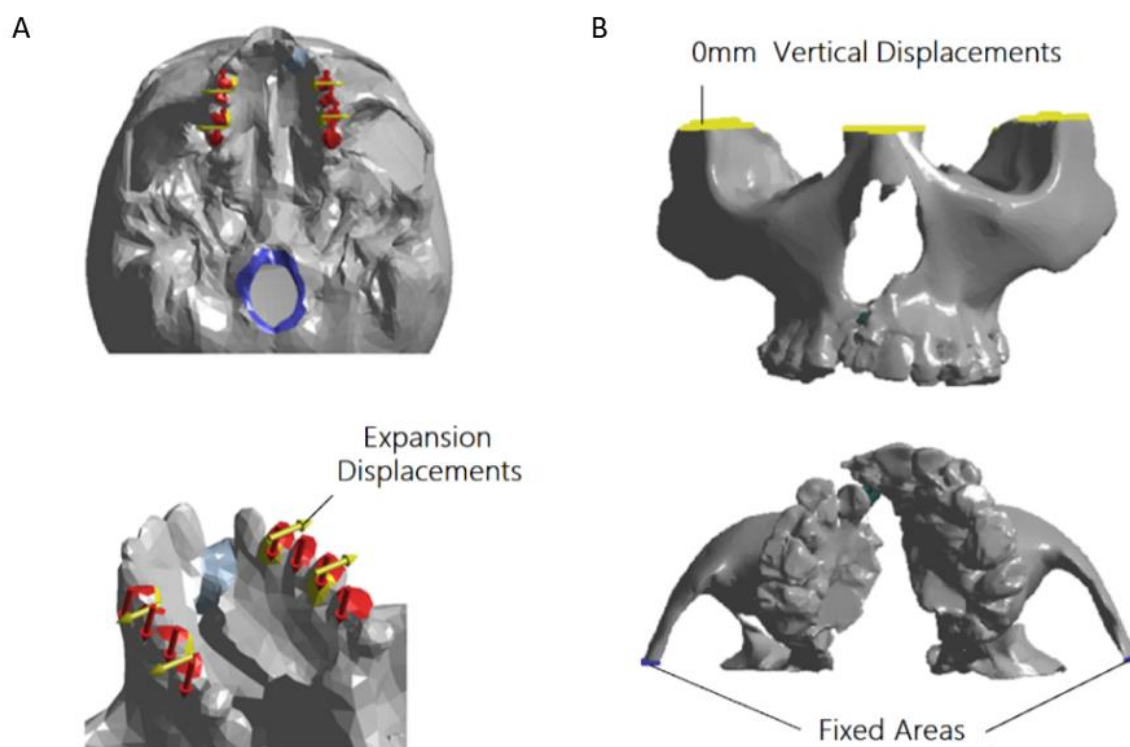
Figure 5.5.1.1 Boundary conditions of A) maxillary expansion and B) Geometry and fixation areas of the Real Cleft model are also shown.

5.5.2 Mechanical Properties

All materials were considered elastic homogeneous, linear, and isotropic. The degree of graft ossification was considered. The simulations were performed using 6 different elasticity modules, shown in Table 5.5.2.1. Different elasticity modules were used in each case of graft osseointegration, employed by Kurniawan 2012.

The entire skull was considered to be a single bone body, as this study does not intend to investigate the effects on periodontal ligaments or dental crowns. Regarding the bone material, its mechanical properties simulate a relationship between cortical and trabecular bone that reflects the actual composition the skull; the modulus of elasticity used was E = 10000 MPa and Poisson's coefficient = 0.3.
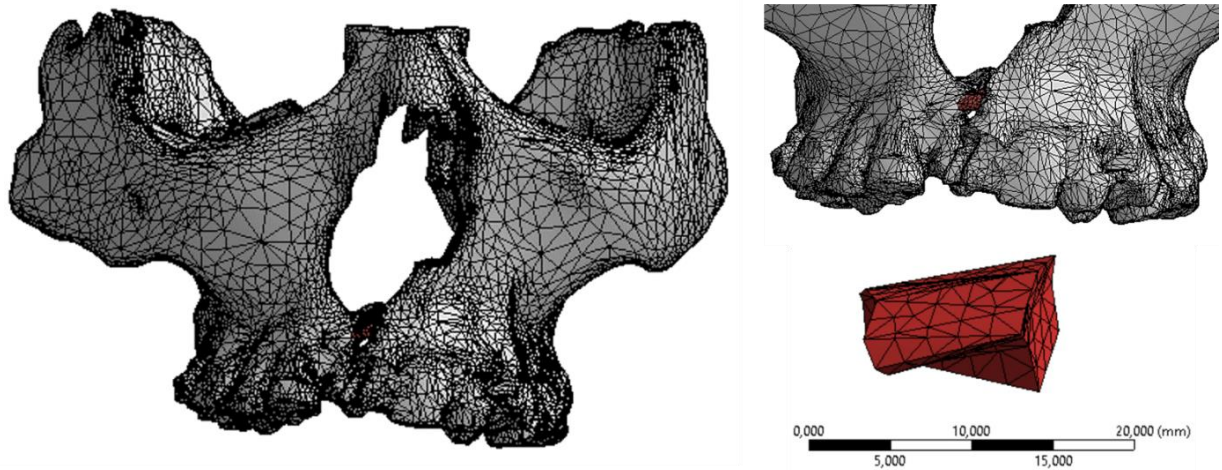
Figure 5.5.2.1 Discretization of the model using 2mm tetrahedral elements in the graft area. A study of the mesh convergence was made to guarantee a good numerical solution.

Table 5.5.2.1 Cases of Real Cleft (RC) and Healthy Skull (HS) models that were simulated. Mechanical properties used in each case are also presented.

Clinical conditions		Simulations	Graft's Mechanical Properties	
RC	Expansion+ Mastication Mastication	50% -100% Ossification of the graft	E50% = 83. 67 MPa E60% = 100. 40 MPa E70% = 117. 13 MPa E80% = 133. 87 Mpa E90% = 150. 60 MPa E100% = 167. 33 MPa	υ=0.3
HS	Expansion+ Mastication Mastication	Skull considered as cortical bone	E cortical = 10000 MPa	υ=0.3
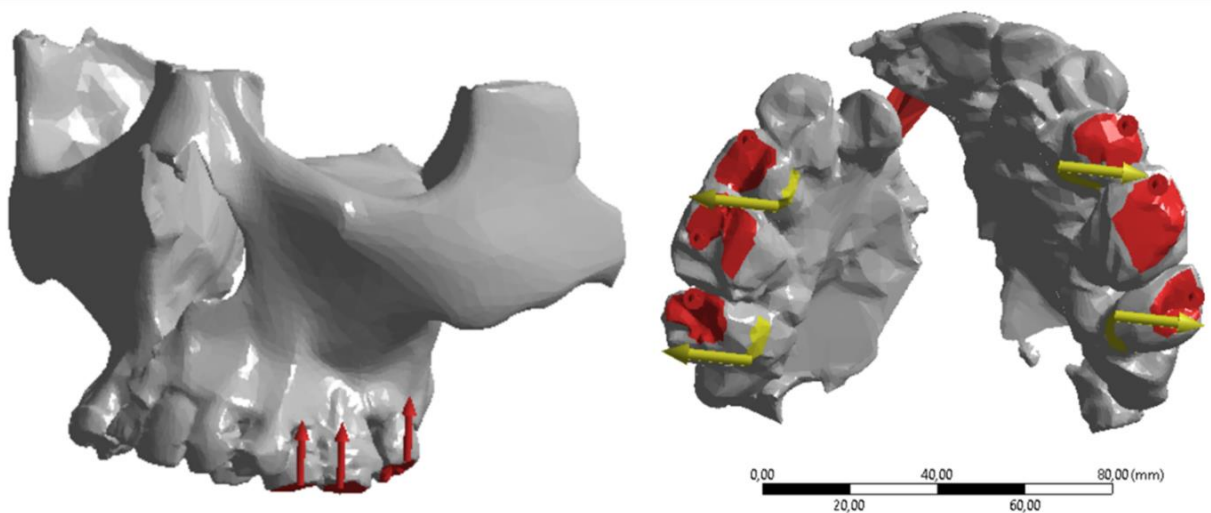
Figure 5.5.2.2 Expansion forces: vectors in red are the chewing forces, vectors in yellow are the displacement of the expansion. Each displacement was equal to 0.125 mm.

6

RESULTS

6.1 Evaluation of the volume and density

A high intra and inter reliability for the density assessments were observed. The inter rater reliability is described in Table 6.1.1. The intra rater reliability is provided in Table 6.1.2 and 6.1.3.

Table 6.1.1. Intraclass Correlation Coefficient (Inter rater reliability)							
		Intraclass Correlation[b]	*95% Confidence Interval*		*F Test with True Value 0*		
			Lower Bound	*Upper Bound*	*Value*	*df1*	*df2*
T1 R1/R2	Landmark 1	.996[c]	0.985	0.999	236.788	9	9
	Landmark 2	.994[c]	0.974	0.998	140.218	9	9
	Landmark 3	.992[c]	0.968	0.998	114.143	9	9
	Landmark 4	.859[c]	0.177	0.968	12.035	9	9
	Landmark 5	.850[c]	0.17	0.966	10.975	9	9
	Landmark 6	.863[c]	0.474	0.966	8.517	9	9
T2 R1/R2	Landmark 1	.939[c]	0.645	0.986	24.543	9	9
	Landmark 2	.933[c]	0.721	0.984	18.204	9	9
	Landmark 3	.932[c]	0.731	0.983	16.898	9	9
	Landmark 4	.886[c]	0.54	0.972	8.192	9	9
	Landmark 5	.938[c]	0.671	0.985	22.643	9	9
	Landmark 6	.802[c]	0.024	0.954	8.383	9	9

Table 6.1.2. Intraclass Correlation Coefficient (Intra- rater reliability_R1)						
		Intraclass Correlation[b]	95% Confidence Interval		F Test with True Value 0		
			Lower Bound	Upper Bound	Value	df1	df2
T1 R1	Landmark 1	.999[c]	0.994	1	1287.038	5	5
	Landmark 2	.996[c]	0.969	0.999	229.597	5	5
	Landmark 3	.993[c]	0.95	0.999	141.765	5	5
	Landmark 4	.996[c]	0.973	0.999	268.534	5	5
	Landmark 5	.997[c]	0.969	1	313.624	4	4
	Landmark 6	1.000[c]	1	1	19279.874	5	5
T2 R1	Landmark 1	.996[c]	0.938	0.999	222.351	5	5
	Landmark 2	1.000[c]	1	1	.	5	5
	Landmark 3	.999[c]	0.994	1	1273.779	5	5
	Landmark 4	1.000[c]	1	1	572394.778	5	5
	Landmark 5	1.000[c]	1	1	.	5	5
	Landmark 6	.999[c]	0.994	1	1208.504	5	5

Table 6.1.3. Intraclass Correlation Coefficient (Intra- rater reliability_R2)						
		Intraclass Correlation[b]	95% Confidence Interval		F Test with True Value 0		
			Lower Bound	Upper Bound	Value	df1	df2
T1 R2	Landmark 1	1.000[c]	1	1	.	5	5
	Landmark 2	1.000[c]	1	1	15047.676	5	5
	Landmark 3	1.000[c]	1	1	33540.876	5	5
	Landmark 4	.999[c]	0.992	1	853.237	5	5
	Landmark 5	.995[c]	0.962	0.999	189.228	5	5
	Landmark 6	1.000[c]	0.999	1	8616.488	5	5
T2 R2	Landmark 1	.999[c]	0.994	1	1140.751	5	5
	Landmark 2	.999[c]	0.994	1	1175.067	5	5
	Landmark 3	.998[c]	0.986	1	497.848	5	5
	Landmark 4	1.000[c]	1	1	30254.699	5	5
	Landmark 5	1.000[c]	1	1	.	5	5
	Landmark 6	1.000[c]	1	1	19473.64	5	5

The volume measurements were assessed at two different times and the descriptive statistics is shown in table 6.1.4.

Volume decreased 54% in T2 (720mm^3, P < .005), however no significate difference was found between our control graft which showed a slightly increase in T2 0.4%(7.5 mm^3, NS).

60 days after surgery the density of the bone graft showed a significant increase of 41% (mean -56.16, P < .005), since the mean values in T1 for lower density (mean 136.17) was lower compared to T2 (mean 192.33).

No significate difference was found for the highest density values between grafts (mean 49.67, -5%, NS) in which T1 had a higher mean (mean 929.16) than T2 (mean 886.33). Table 6.1.5 shows the T-Test results.

Table 6.1.4 Descriptive (average values)				
	Minimum	Maximum	Mean	Std. Deviation
Graft T1_Volume (mm3)	1226.5	1412	1331.7	101.2
Graft T2_Volume (mm3)	579.5	666	611.7	47.3
Control T1 volume (mm3)	180.5	199.5	188.7	9.9
Control T2_volume (mm3)	188	205.5	196.2	8.8
Graft T1_Lower_bone density	102	157	136.1	30.0
Graft T2_Lower_bone density	137.5	235	192.3	50.8
Graft T1_Upper_bone density	826	1008	929.1	95.2
Graft T2_Upper_bone density	704.5	1076	886.3	208.5

Table 6.1.5 T-TEST mean difference between T1 and T2					
	Mean	Std. Deviation	Std. Error Mean	% error	Sign.
Volume (Graft)	720	80.165	32.727	-54%	*
Lower density values	-56.167	67.378	27.507	41%	*
Upper density values	-49.667	247.344	100.978	-5%	NS
volume (control)	-7.5	12.582	5.136	4%	NS

6.2 Animal Results

The results demonstrated that the autogenous bone graft assisted the reconstruction of the neoformed bone in the maxillary defect of the mouse and was also confirmed with the histological slides photographed.

We can observe in the slides photographs that the bone fragments containing osteocytes contributed to a higher bone formation activity; however, fourteen days after surgery, there was a resorption of the smaller fragments of bone, which shows in the results of micro CTs that there was a resorption at this stage. What can also be observed is that, after 21 days of the surgery, the graft side had a much higher ossification than the non-graft side, due to the presence of bone spicules with osteocytes, and the presence of bone graft osteoblasts originated from the grafted bone.

It was observed that, after 24 hours, 7, 14 and 21 days, the bone graft side presented higher bone mineral density (BMD, g/cm3), percentage of bone volume (BV/TV%) and bone volume (BV, mm3) in comparison to the non-grafted side. Dashed line represents the data of the control animals, without simulation of fissure bone and/or bone graft (Figs. 6.2.1, 6.2.2, 6.2.3 and 6.2.4).
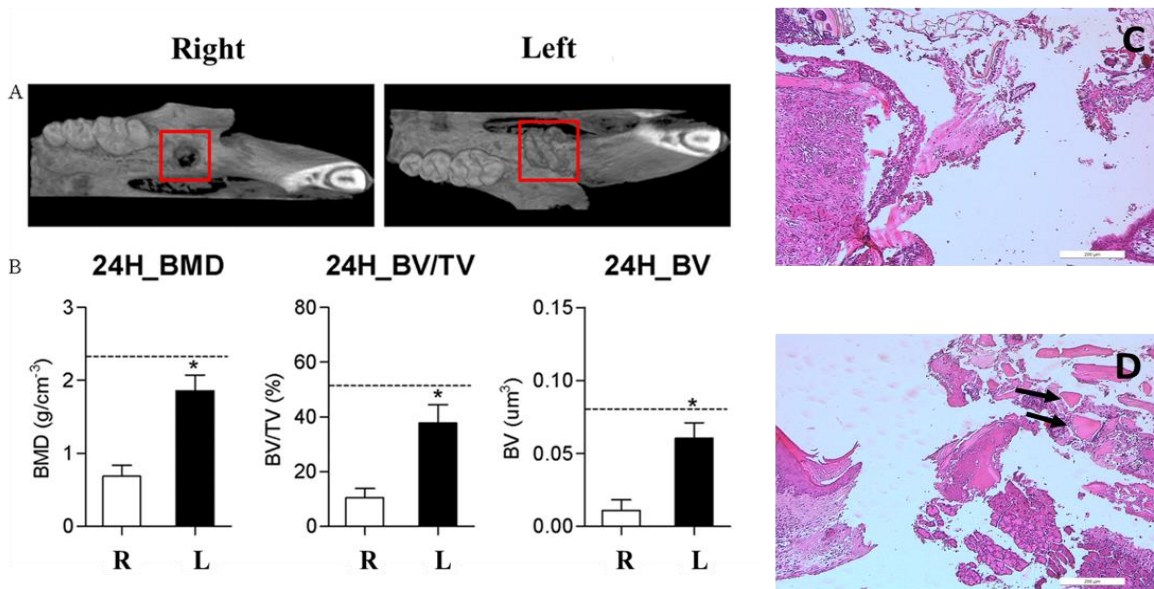
Figure 6.2.1 A) Comparison for 24 hours after of the surgery in the maxilla of the mouse, between the right side of the maxilla, where there was no osseous graft and the left side, where there was an osseous graft. B) Micro–computed tomography (micro CT) results. Micro CT parameters: bone mineral density (BMD, g/cm3), percent bone volume (BV/TV %), bone volume (BV, mm3). Five mice were used per group. Statistical analyses performed by Student's t-test. * p <0.05 different from right side. C) Histological slide without bone graft. D) Histological slide with bone graft, the arrows show the spicules of the bone scraped.
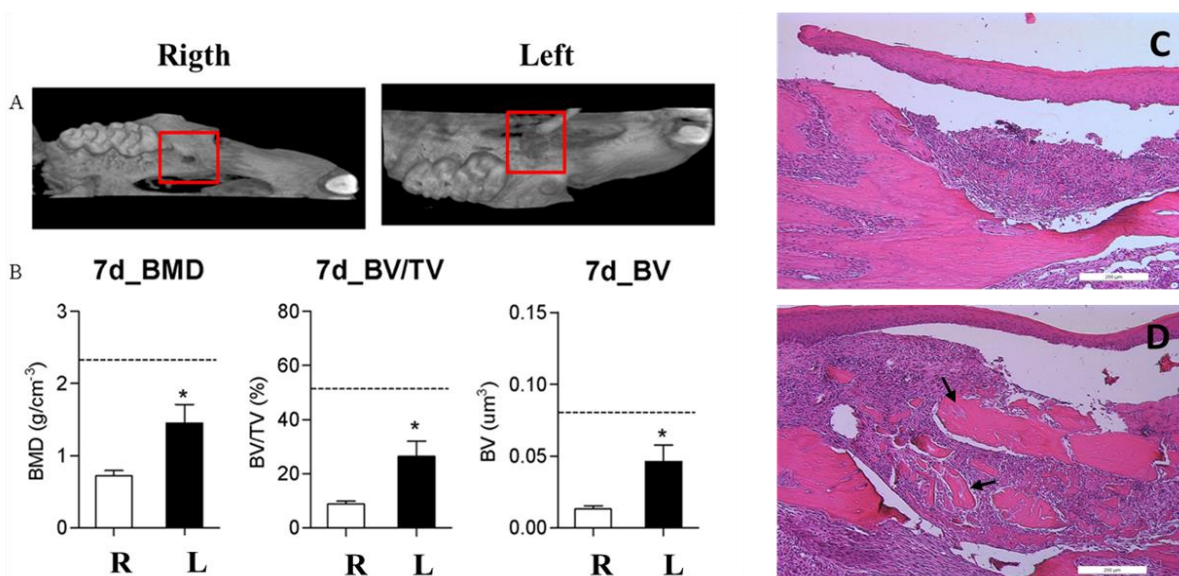
Figure 6.2.2 A) Comparison 7 days after of the surgery in the maxilla of the mouse, between the right side of the maxilla, where there was no osseous graft and the left side, where there was an osseous graft. B) Micro–computed tomography (micro CT) results. Micro CT parameters:

bone mineral density (BMD, g/cm3), percent bone volume (BV/TV %), bone volume (BV, mm3). Five mice were used per group. Statistical analyses performed by Student's t-test. * p <0.05 different from right side. C) Histological slide without bone graft. D) Histological slide with bone graft.
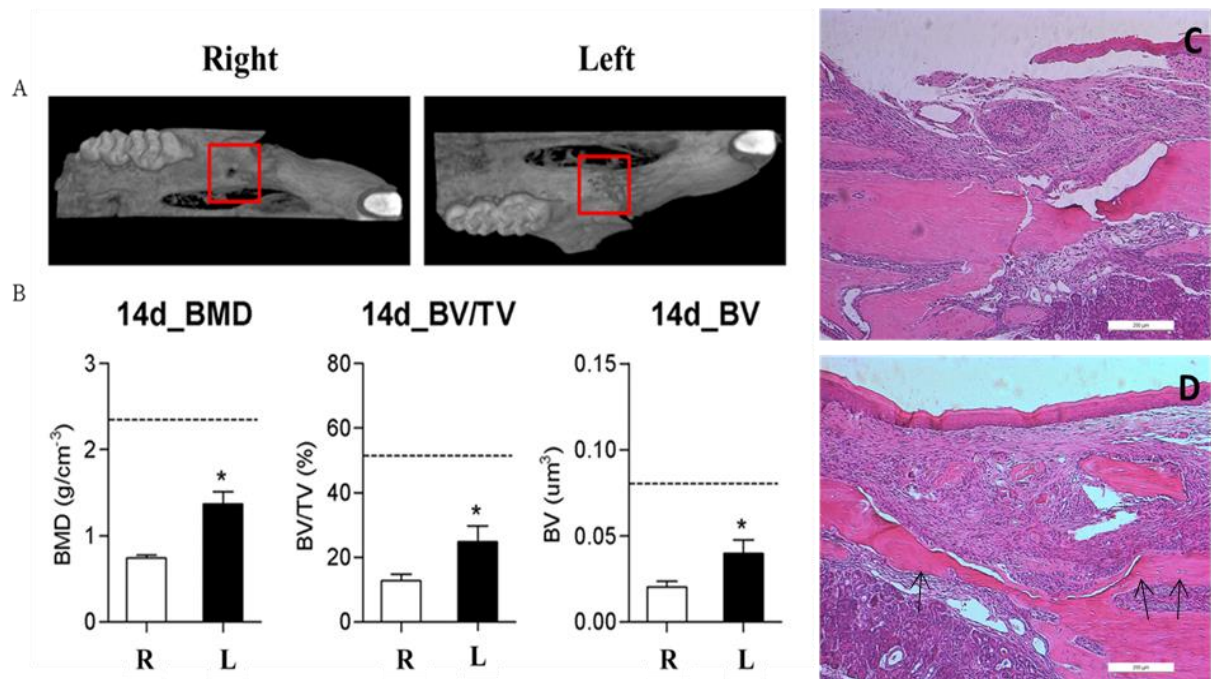
Figure 6.2.3 A) Comparison 14 days after of the surgery in the maxilla of the mouse, between the right side of the maxilla, where there was no osseous graft and the left side, where there was an osseous graft. B) Micro–computed tomography (micro CT) results. Micro CT parameters: bone mineral density (BMD, g/cm3), percent bone volume (BV/TV %), bone volume (BV, mm3). Five mice were used per group. Statistical analyses performed by Student's t-test. * p <0.05 different from right side. C) Histological slide without bone graft. D) Histological slide with bone graft, the arrows show the osteocytes migration for the new bone formation.
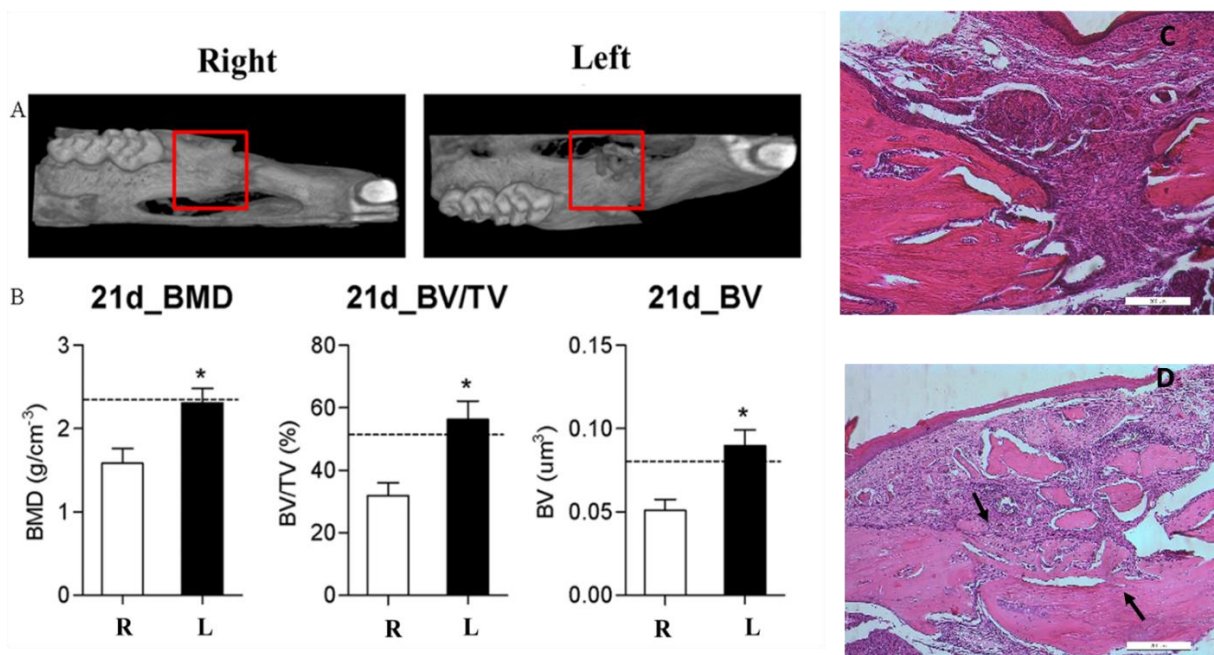
Figure 6.2.4 A) Comparison 21 days after of the surgery in the maxilla of the mouse, between the right side of the maxilla, where there was no osseous graft and the left side, where there was an osseous graft. B) Micro–computed tomography (microCT) results. MicroCT parameters: bone mineral density (BMD, g/cm3), percent bone volume (BV/TV %), bone volume (BV, mm3). Five mice were used per group. Statistical analyses performed by Student's t-test. * p <0.05 different from right side. C) Histological slide without bone graft. D) Histological slide with bone graft, the arrows show the new bone formation.

Except for the BMD in the period of 24 hours, the analysis of the timeline results demonstrated that there was significant reduction in bone formation, represented by the decrease in BMD, BV/TV and BV in the period of 24 hours, 7 and 14 days compared to the period of 21 days in both sides, grafted and non-grafted. The analyzes performed 21 days after surgery showed a significant bone neoformation on the grafted side, reaching the expected levels of neoformed bone represented by the dashed line of the control group (Fig. 6.2.5).
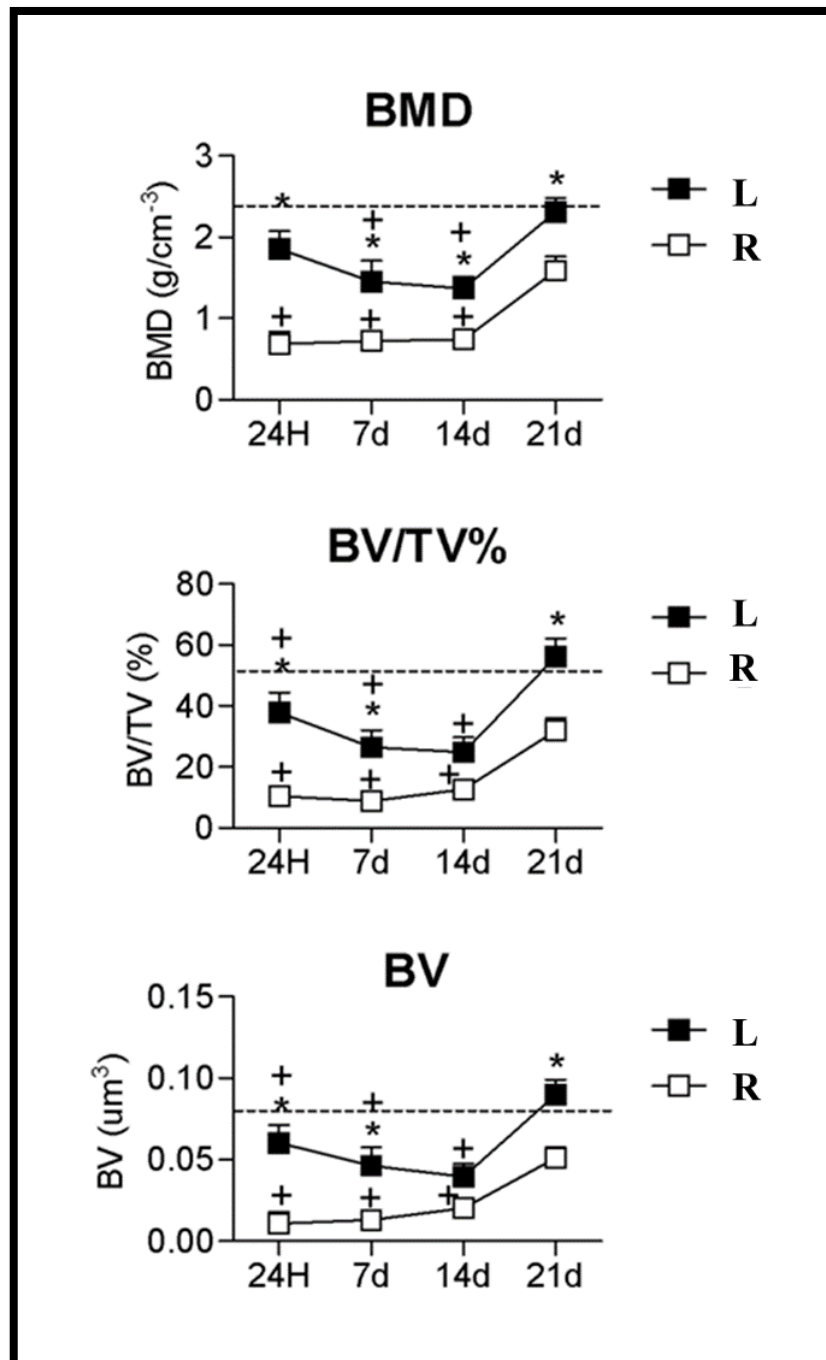
Figure 6.2.5 Comparison between all groups with microCT parameters: bone mineral density (BMD, g/cm3), percent bone volume (BV/TV %), bone volume (BV, mm3). Five mice were used per group. Statistical analyses performed by Student's t-test. + $p < 0.05$ different from the period of 21 days; +* $p < 0.05$ different from the right side.

We can conclude that the autogenous bone graft plays an important role in the formation of a new bone, showing efficacy in the bone regeneration comparing the maxilla side with bone graft, to the control side without bone graft.

6.3 Biomechanical results

6.3.1 Healthy skull model

The distribution of MPS in health model under the 2 clinical conditions suggests that stresses are higher when the skull is solely exposed to maxillary expansion than when it is solely exposed to mastication forces, as shown in Fig. 6.3.1.

This result was obtained in both the cleft and the healthy skulls. Mastication stresses are lower compared to the clinical condition of maxillary expansion with orthopedic therapy. On the other hand, Fig. 6.3.1 shows that the stress distribution in the healthy skull was symmetrical, as expected.

For maxillary expansion, stresses on the palate seem to be greater in the healthy skull. However, this result should be treated with caution since the presence of the medial palatal suture is not considered in the model (Vélez Muriel 2020).
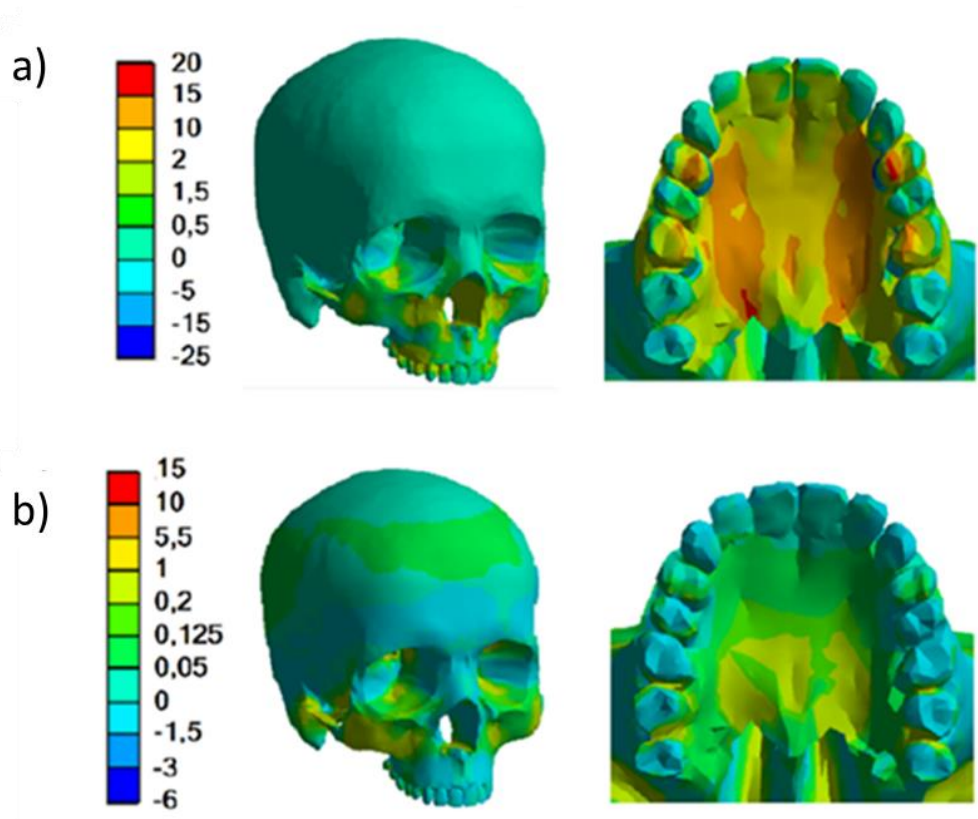
Figure 6.3.1 Maximum principal stress (MPS) distribution in a healthy skull model under a) maxillary expansion; and b) mastication conditions. All stresses are in MPa.

6.3.2 Cleft model

Results of the Cleft model with a 50% ossified graft under expansion conditions are shown in Fig. 6.3.2. Expansion results of MPS at the frontal face of the graft are around 0.05 MPa. Also, stresses in the palate show values, between 0.5 and 0.3 MPa. The overall stress distribution shows some increased results at the eye cavities and at regions where boundary conditions were applied in each model.

As for expansion, results of stresses in the Cleft models are presented in Fig. 6.3.2.1. The global stress distributions are very alike, showing increased stress results around the zygomatic bone -below the eye cavities. Regarding graft and the palate, results are about 1 and 4 MPa, respectively. Fig. 6.3.2.2 shows maximum principal, shear and hydrostatic stresses obtained along zone 1 in the Cleft model. The x axis of the figures corresponds to the horizontal position of the points along zone 1. Each line represents a certain degree of graft ossification. The behavior of these results is expected since the stresses increase in the graft and its surrounding areas, and they also increase as the graft ossifies.
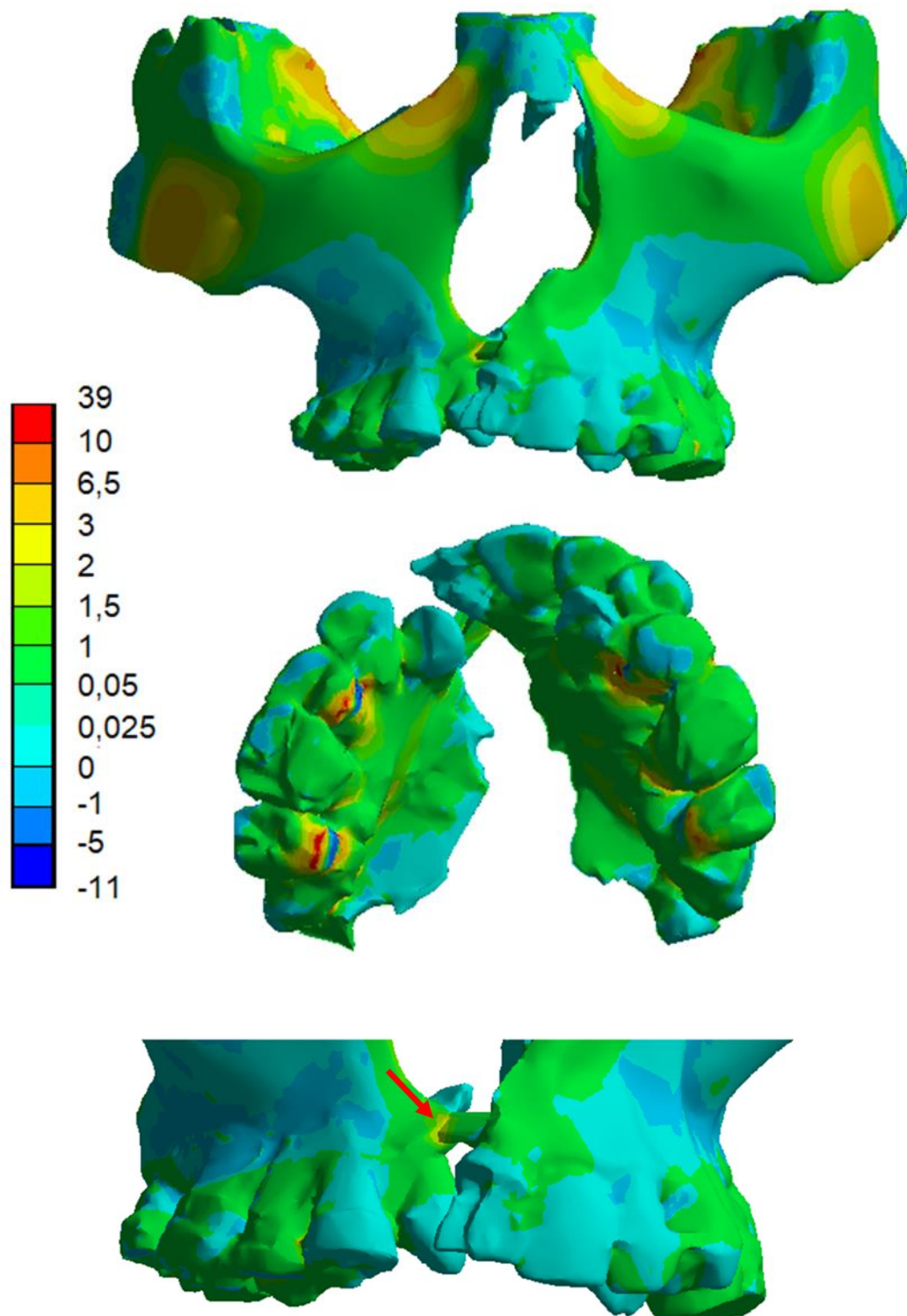
Figure 6.3.2.1 Maxillary expansion results obtained in the Cleft model. Figure corresponds to results obtained with 50% of graft ossification. Stresses are in MPa. The arrow shows the area where the stresses intensify when the cleft expands.
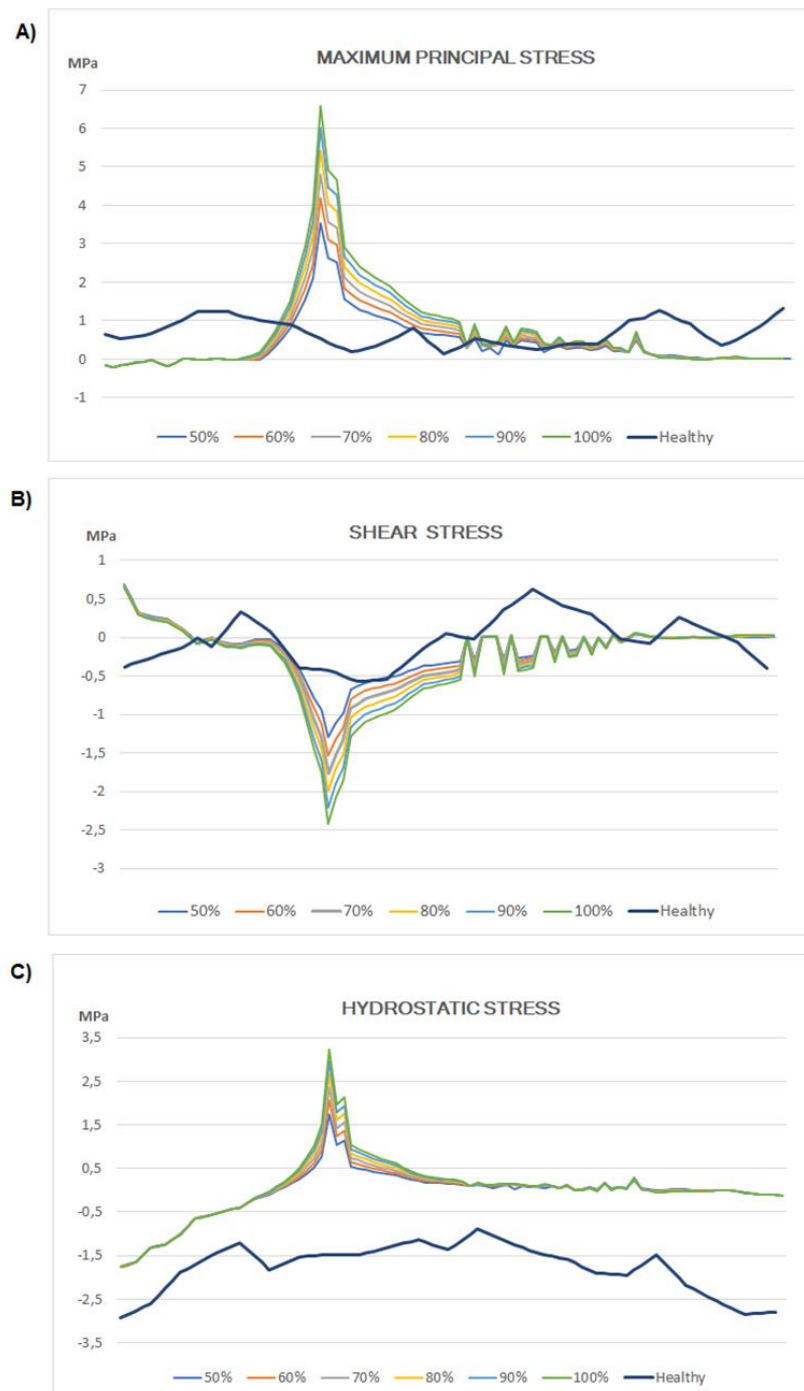
Figure 6.3.2.2 a) MPS, b) shear and c) hydrostatic stresses caused by Expansion forces in the Cleft model, along zone 1. Results of the Healthy Skull model (HS) are also shown.

A comparison of the absolute value of maximum principal, shear and hydrostatic stresses due to maxillary expansion and mastication loads in Real Cleft and Health Skull is presented in Fig. 6.3.2.3.

For Real Cleft geometries, MPS with the graft seem to vary less than 0.5 MPa from one geometry to the other, corresponding to about 15%. The results suggest that a health skull will undergo lower stresses when compared with skulls with palatal clefts. Additionally, the expansion therapy in both healthy and cleft skulls increase stresses compared with skulls with just mastication forces.
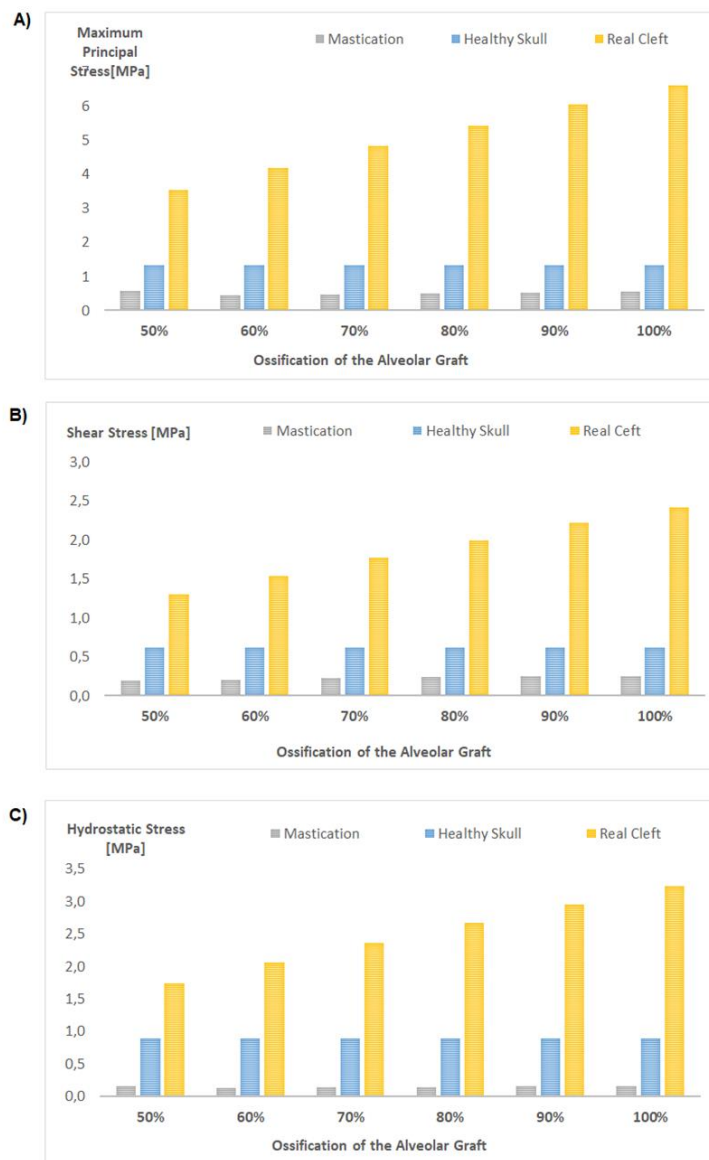
Figure 6.3.2.3 Comparison of a) maximum principal, b) shear and c) hydrostatic stresses between the cleft and healthy models under maxillary expansion clinical condition.

Maximum Principal Stress of the graft: the results were calculated with the graft elasticity
Module equal to 167,33 MPa.
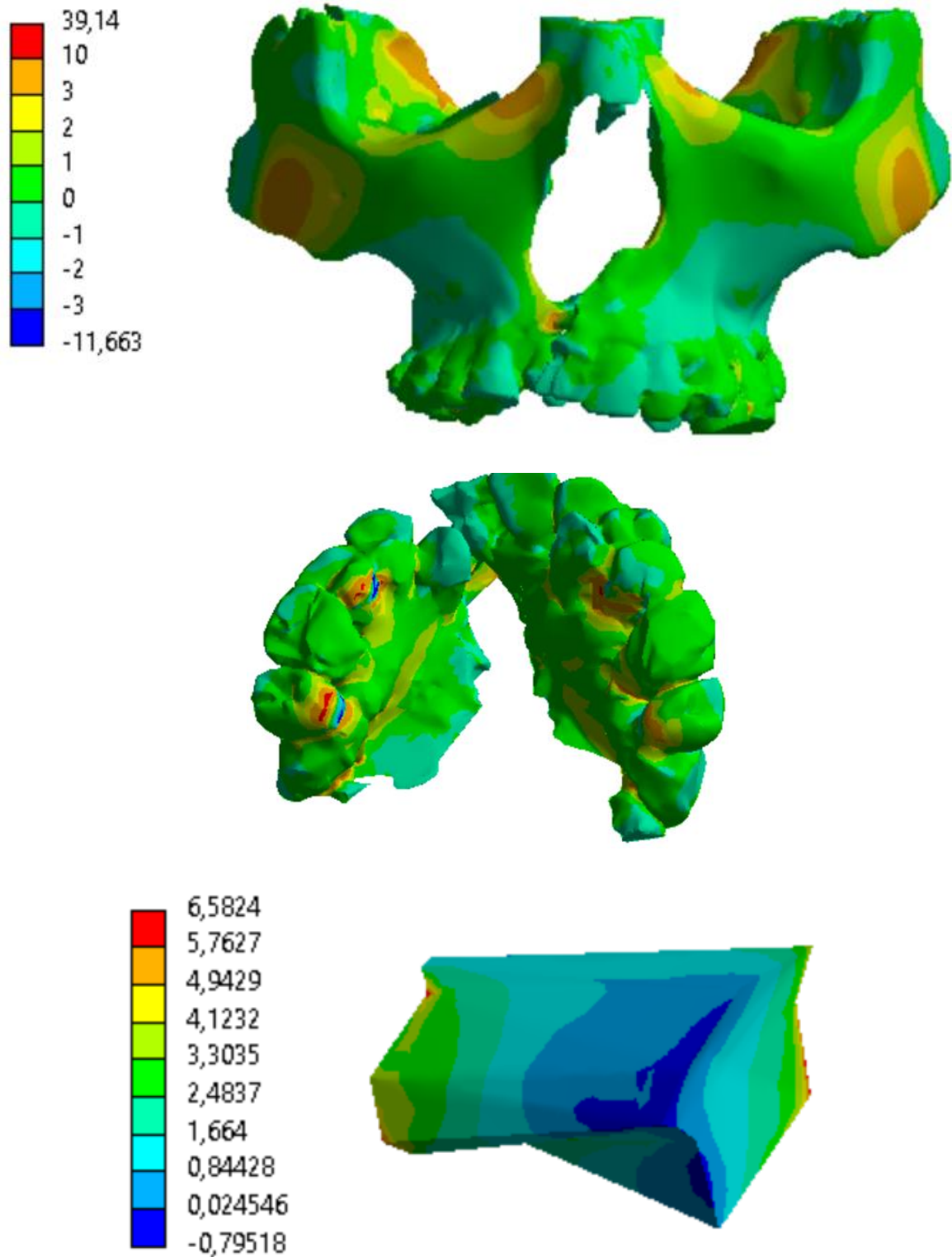
Figure 6.3.2.4 Graft model, the stress increase where are in contact of the periosteum and
decrease in the middle of the graft.

6.3.3 Validation of the FEM

FEM stresses results in the graft show an increase in the left wall of the graft, then a decrease in the middle where maximum principal stresses equal to 0 MPa, and finally a lightly increase in the right wall of the graft where stresses reach -1 MPa. The negative sign of the last result means that the graft is subjected to compression forces instead of traction forces.

The comparison of these MEF with the clinical result at T2 (60 days after surgery), shown in Fig. 6.3.3.1, that the absence of tension in the middle of the graft coincides with the area where the graft reabsorption occurred in the clinical environment. This comparison is an indication of the reliability of the model to reproduce the clinical outcome.
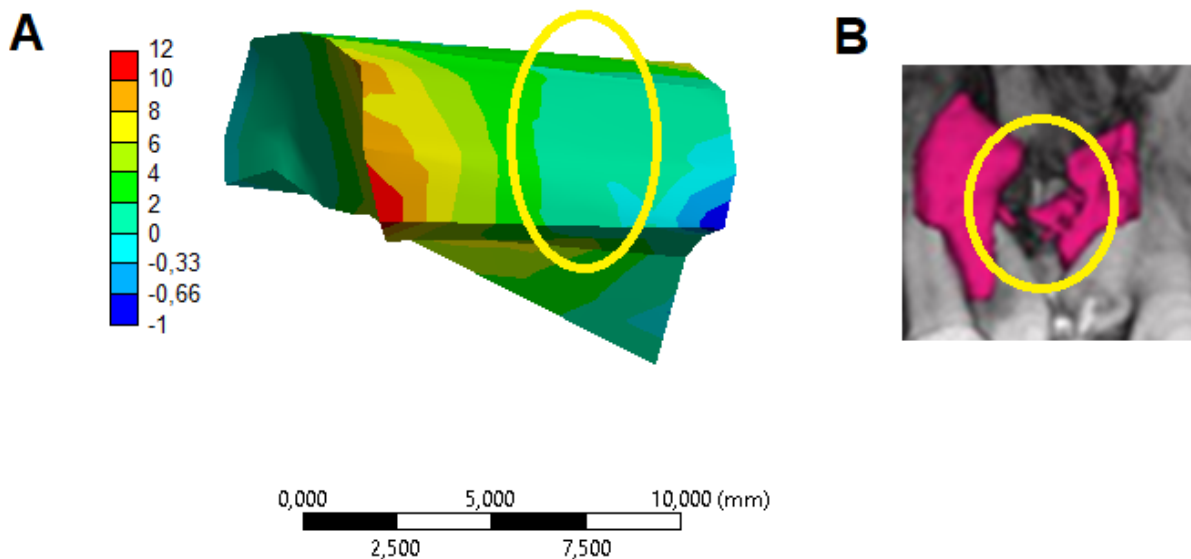
Figure 6.3.3 Comparison of A) FEM results and b) clinical results of the graft at T2.

7

DISCUSSION

The "gold standard" technique is the use of bone grafts in patients between 9 and 12 years old, with a high success rate confirmed by several studies (Boland et al.,2009). The main reason is the eruption to the canines, which occurs around this age, subjecting the graft to mechanical and biological stimuli, which favor graft to became a new bone.

According to Feichtinger et al. 2008, in their study, the bone loss of graft was 57% after one year, however, the residual bone bridges had increased in volume as a response to erupting canine.

In this study, the patient lost the best age to undergo bone graft surgery, which often leads to failure due to lack of physiological stress. As a replacement to this physiological factor, the proposal is to generate stress with maxillary expansion, using the Hyrax orthodontic appliance.

The volume and density differences were evaluated in graft bone of a cleft lip patient between 15 days and 60 days after surgery. A high reliability between assessments was observed, and both decrease in volume and increase in density was observed in 60 days after surgery compared to 15 days.

The percentage of decreased volume in our study was around 54% of the graft in 60 days, which is higher than a previous CBCT study in which a reabsorption of 43% was observed in the first year (Tai, Sutherland, & McFadden, 2000). This difference may be due to the difference technique to measure the volume.

The Hounsfield unit (HU) is used by radiologists to interpretation of a relative quantitative measurement of radio density of CT images. In CBCT the grey-values are Image reconstruction software associate a CT number to each voxels size, in Dolphin HU's values was assessed to determine the bone density. It is important to say that Dolphin HU's values, differs from CT

HU's values, and also CT HU's values may not be the same even when the same CT machine is used.

However, in this specific study, we did not observe significant difference between our controls, consequently absence of significant difference between the scanners. Therefore, either no difference between scanners parameters was observed even though the CBCT's were taken in difference times, or if the scanning protocol was different, the difference did not interfere in the results.

Volume measurements can also have some variation due to the scanning parameters that affect the measured density values and the HU cut off values.(Thereza-Bussolaro et al. 2020) Nevertheless, no difference was observed in our control, thus obtained volume results shows graft volume decreased from T1 to T2.

In T1, the higher mean value for upper density values, and the lowest mean value for lower density. We were expecting to observe this behavior, since this type of autologous graft has in its composition a variety of bone density compounds, ranging from very low density and high density iliac crest spicules. This result was expected since it is known that after the placement of the graft, bone remodeling process begins with bone resorption (García et al. 2008) and then lead to osseous integration of the graft and the synthesis of new bone material.

Consequently, due to the maturation process in the 60 days, we observed higher mean value for lower density, although not higher value for the upper density, which can be explained by the bone remodeling of the spicules and the formation of the new bone, that have lower density that a mature bone.

In the biological process of bone formation, resorption of the old bone tissue occurs first, and then a new bone is formed (Mandalunis 2006).

At the experiment with the mice, it was observed that a resorption of the bone graft spicules occurs until 14 days after surgery, and 21 days after the surgery it was observed a new bone formation on the basis (Fig. 5.3.4.1). Figure 6.5.2 shows that bone mineral density and the bone volume on the bone graft side decreased until 14 days, and with 21 days the bone density and the volume increased considerably.

Regarding the fact that bone resorption is expected as a biological phenomenon, in this study we tried to obtain the best time to apply load to stimulate bone neoformation. Many studies

show that loading increases bone formation and suppresses bone resorption (Fernández et al. 2006 and Ralston 2017).

It was possible to analyze the density and volume of the bone graft of patient A.S. and we observed that the bone graft with almost 15 days was present in high volume and low density. However, after 60 days, 54% of the bone graft was absorbed and the density of the new bone was less than that of a normal bone (Fig. 5.2.7).

Based on this observation, the best time to activate the Hyrax device and expand the maxilla of the A.S. patient should be between 15 and 20 days after bone graft surgery, as we still have a large volume of ground bone and the osteoblasts alive. Maxillary expansion after bone graft surgery can be performed as reported in Cavassan et al. 2004.

The mechanical expansion caused by the Hyrax device, after graft surgery, can strengthen the bone reconstruction process in patients with cleft palate. According to Sun et al. 2018, the bone resorption process occurs first, then, through the effect of osteoclasts, osteoblasts are activated to produce new bone. This mechanical stimulation promotes an improvement in bone remodeling of the graft.

The biomechanics models simulated in the present study show that the stress values found when maxillary expansion forces were applied promotes a positive stimulus to increase bone formation, reaching about 6.5 MPa in trabecular bone.

However, the peak of stresses in figure 5.4.3, along the zone 1, shows that as the modulus of elasticity of the graft increases, the maximum principal, shear and hydrostatic stresses also increase in the cleft model when compared with the health skull model.

This is because the greater the modulus of elasticity, the greater the stiffness of the structure. The stiffness is defined as stress / strain, an increase in stiffness implies in an increase in the forces necessary to deform the structure (Baumgart, F., 2000). A bone with higher degree of osseointegration bears higher stresses and lower strains (Kurniawan, Denni et al., 2012).

According to Tokugawa 2012, the zones nearby the cleft are denser, this suggest that the mechanical stimuli in the graft start in the areas that are in contact with other tissues, such as the periosteum and alveolar bone. Related to this, according to Dissaux 2016, the graft resorption occurs mainly in the sagittal dimension - middle part of the graft. This phenomenon varies the graft volume in areas far from other tissues.

Following the biomechanical behavior of the bone graft for patient A.S., analyzing the results of the Dolphin program (Fig.5.2.7) and comparing it with the FE results of the bone graft (Fig.5.4.5), it can be observed that there is less stress in the middle of the bone graft, where the greatest bone resorption occurs, suggesting that the mechanical stimuli in the graft start in the areas that are in contact with the patient's palatal bone, where the stimuli on the graft begins.

The clinical case reported in this work, patient A.S., used the traditional treatment protocol, where the maxilla is expanded before bone graft surgery, and showed 54% of resorption in the first month. This is in line with the results of (FEICHTINGER, Matthias et al., 2008), who showed that the means bone loss was 51% in the first and 52% in the second year.

Bone graft success is multifactorial, and specific causal elements cannot be identified in this type of study. A limited sample of only one clinical case, which was analyzed for the construction of biomechanical models, without clinical application of the results, is a limitation of this study. This is a deeper look at the mechanical stimuli in the graft. Further studies are needed to verify the new clinical technique suggested. However, the finding of the present study suggests clinically relevant data on the possibility of the stimulatory effect of expansion stresses on late bone graft in adult patients with cleft palate.

8

CONCLUSION

Biomechanical models can be used to determine deformations and stresses in the area of the bone graft. These results serve for a holistic analysis of biological processes; such as bone resorption.

The present work suggests that the use of the Hyrax appliance is effective for patients who have lost their best age after bone graft surgery. Activation of Hyrax between 15 and 20 days after surgery would mechanically stimulate the graft, increasing the success rate of the procedure.

The comparison of MEF results with the clinical result of the CBCT, 60 days after the surgery, validated that the low level of stresses in the middle of the graft coincides with the area where the graft reabsorption occurred.

Despite the limitations of this study, the results support a change in the treatment protocol for adult patients with cleft palate.

9

REFERENCES

ANDRADE JR, I. et al. CCR5 down-regulates osteoclast function in orthodontic tooth movement. Journal of dental research, v. 88, n. 11, p. 1037-1041, 2009.

ANGELL, D. H. Treatment of irregularity of the permanent or adult teeth. Dent. Cosmos, v. 1, p. 540-544, 1860.

BAUMGART, F. Stiffness-an unknown world of mechanical science?. Injury-International Journal for the Care of the Injured, v. 31, n. 2, p. 14-23, 2000.

BERGLAND, Olav et al. Secondary bone grafting and orthodontic treatment in patients with bilateral complete clefts of the lip and palate. Annals of plastic surgery, v. 17, n. 6, p. 460-474, 1986.

BERGLAND, Olav; SEMB, Gunvor; ABYHOLM, Frank E. Elimination of the residual alveolar cleft by secondary bone grafting and subsequent orthodontic treatment. The Cleft palate journal, v. 23, n. 3, p. 175-205, 1986.

BICKLER, Stephen W. et al. Global burden of surgical conditions. Disease control priorities, v. 1, p. 19-40, 2015.

BOLAND, F.-X. et al. Gingivopériostoplasties associées à une greffe osseuse: évaluation radiologique. Revue de Stomatologie et de Chirurgie Maxillo-faciale, v. 110, n. 4, p. 193-197, 2009.

BOUXSEIN, Mary L. et al. Guidelines for assessment of bone microstructure in rodents using micro–computed tomography. Journal of bone and mineral research, v. 25, n. 7, p. 1468-1486, 2010.

BOYNE, Philip J. Secondary bone grafting of residual alveolar and palatal clefts. J Oral Surgery, v. 30, p. 87-92, 1972.

BOYNE, Philip J.; SANDS, Ned R. Combined orthodontic-surgical management of residual palato-alveolar cleft defects. American journal of Orthodontics, v. 70, n. 1, p. 20-37, 1976.

CAMPBELL, Graeme M.; SOPHOCLEOUS, Antonia. Quantitative analysis of bone and soft tissue by micro-computed tomography: applications to ex vivo and in vivo studies. BoneKEy reports, v. 3, 2014.

CARANO, Richard AD; FILVAROFF, Ellen H. Angiogenesis and bone repair. Drug discovery today, v. 8, n. 21, p. 980-989, 2003.

CARTER, Dennis R. Mechanical loading histories and cortical bone remodeling. Calcified tissue international, v. 36, n. 1, p. S19-S24, 1984.

CARVALHO TROJAN, Larissa et al. Stresses and strains analysis using different palatal expander appliances in upper jaw and midpalatal suture. Artificial organs, v. 41, n. 6, p. E41-E51, 2017.

CHAKKALAKAL, D. A. et al. Repair of segmental bone defects in the rat: an experimental model of human fracture healing. Bone, v. 25, n. 3, p. 321-332, 1999.

CHEONG, Vee San et al. A novel adaptive algorithm for 3D finite element analysis to model extracortical bone growth. Computer methods in biomechanics and biomedical engineering, v. 21, n. 2, p. 129-138, 2018.

CHOU, Hsuan-Yu; MÜFTÜ, Sinan. Simulation of peri-implant bone healing due to immediate loading in dental implant treatments. Journal of biomechanics, v. 46, n. 5, p. 871-878, 2013.

CLARK, D. P.; BADEA, C. T. Micro-CT of rodents: state-of-the-art and future perspectives. Physica Medica, v. 30, n. 6, p. 619-634, 2014.

COHEN, M.; POLLEY, J. W.; FIGUEROA, A. A. Secondary (intermediate) alveolar bone grafting. Clinics in plastic surgery, v. 20, n. 4, p. 691-705, 1993.

DA SILVA FILHO, Omar Gabriel et al. Secondary bone graft and eruption of the permanent canine in patients with alveolar clefts: literature review and case report. The Angle Orthodontist, v. 70, n. 2, p. 174-178, 2000.

DANIELSSON, Per-Erik. Euclidean distance mapping. Computer Graphics and image processing, v. 14, n. 3, p. 227-248, 1980.

DAVAMI, Kamran et al. Long term skeletal and dental changes between tooth-anchored versus Dresden bone-anchored rapid maxillary expansion using CBCT images in adolescents: Randomized clinical trial. International orthodontics, v. 18, n. 2, p. 317-329, 2020.

DEWINTER G, QUIRYNEN M, HEIDBUCHEL K, VERDONCK A, WILLEMS G, CARELS C. 2003. Dental abnormalities, bone graft quality, and periodontal conditions in patients with unilateral cleft lip and palate at different phases of orthodontic treatment. Cleft Palate Craniofac J. 40(4):343-350.

DISSAUX, Caroline et al. Evaluation of success of alveolar cleft bone graft performed at 5 years versus 10 years of age. Journal of Cranio-Maxillofacial Surgery, v. 44, n. 1, p. 21-26, 2016.

DIXON MJ, MARAZITA ML, BEATY TH, MURRAY JC. 2011. Cleft lip and palate: Understanding genetic and environmental influences. Nat Rev Genet. 12(3):167-178.

DOBLARÉ, M.; GARCIA, J. M.; GÓMEZ, M. J. Modelling bone tissue fracture and healing: a review. Engineering Fracture Mechanics, v. 71, n. 13-14, p. 1809-1840, 2004.

ELHADDAOUI, Rajae et al. Calendrier de la greffe osseuse et séquences d'éruption canine dans les cas de fentes labio-alvéolo-palatines: revue systématique. L'Orthodontie Française, v. 88, n. 2, p. 193-198, 2017.

EPPLEY, Barry L.; SADOVE, A. Michael. Management of alveolar cleft bone grafting—state of the art. The Cleft palate-craniofacial journal, v. 37, n. 3, p. 229-233, 2000.

ERICA ALEXANDRA, Macedo Pessoa et al. Alveolar bone graft: clinical profile and risk factors for complications in oral cleft patients. The Cleft Palate-Craniofacial Journal, v. 54, n. 5, p. 530-534, 2017.

FEICHTINGER, Matthias et al. Three-dimensional evaluation of secondary alveolar bone grafting using a 3D-navigation system based on computed tomography: a two-year follow-up. British Journal of Oral and Maxillofacial Surgery, v. 46, n. 4, p. 278-282, 2008.

FEICHTINGER, Matthias; MOSSBÖCK, Rudolf; KÄRCHER, Hans. Assessment of bone resorption after secondary alveolar bone grafting using three-dimensional computed tomography: a three-year study. The Cleft palate-craniofacial journal, v. 44, n. 2, p. 142-148, 2007.

FEICHTINGER, Matthias; MOSSBÖCK, Rudolf; KÄRCHER, Hans. Evaluation of bone volume following bone grafting in patients with unilateral clefts of lip, alveolus and palate using a CT-guided three-dimensional navigation system. Journal of Cranio-Maxillofacial Surgery, v. 34, n. 3, p. 144-149, 2006.

FERNÁNDEZ TRESGUERRES, Isabel et al. Physiological bases of bone regeneration II: The remodeling process. 2006.

FLECKENSTEIN, Peter; TRANUM-JENSEN, Jørgen. Anatomy in diagnostic imaging. John Wiley & Sons, 2014.

FROST, Harold M. Wolff's Law and bone's structural adaptations to mechanical usage: an overview for clinicians. The Angle Orthodontist, v. 64, n. 3, p. 175-188, 1994.

GUYTON, Arthur; HALL, John E. Tratado de Fisiologia Médica (9º Edição). Ed. Guanabara Koogan: Rio de Janeiro, 1997.

HILDEBRAND, Tor; RÜEGSEGGER, Peter. A new method for the model-independent assessment of thickness in three-dimensional images. Journal of microscopy, v. 185, n. 1, p. 67-75, 1997.

HOUNSFIELD, Godfrey N. Computerized transverse axial scanning (tomography): Part 1. Description of system. The British journal of radiology, v. 46, n. 552, p. 1016-1022, 1973.

JIA, Y. L.; FU, M. K.; MA, L. Long-term outcome of secondary alveolar bone grafting in patients with various types of cleft. British Journal of Oral and Maxillofacial Surgery, v. 44, n. 4, p. 308-312, 2006.

JUNQUEIRA, L. C.; CARNEIRO, J. Histologia Básica. 10 a edição ed. 2004.

KALAAJI, A. et al. Bone grafting in the mixed and permanent dentition in cleft lip and palate patients: long-term results and the role of the surgeon's experience. Journal of Cranio-Maxillofacial Surgery, v. 24, n. 1, p. 29-35, 1996.

KAPPEN I, BITTERMANN GKP, BITTERMAN D, MINK VAN DER MOLEN AB, SHAW W, BREUGEM CC. 2017. Long-term follow-up study of patients with a unilateral complete cleft of lip, alveolus, and palate following the utrecht treatment protocol: Dental arch relationships. J Craniomaxillofac Surg. 45(5):649-654.

KATSUMATA, Akitoshi et al. Effects of image artifacts on gray-value density in limited-volume cone-beam computerized tomography. Oral Surgery, Oral Medicine, Oral Pathology, Oral Radiology, and Endodontology, v. 104, n. 6, p. 829-836, 2007.

KAWALEC, Agata et al. Risk factors involved in orofacial cleft predisposition–review. Open Medicine, v. 10, n. 1, 2015.

KAZEMI, Amin; STEARNS, Jeffrey W.; FONSECA, Raymond J. Secondary grafting in the alveolar cleft patient. Oral and Maxillofacial Surgery Clinics, v. 14, n. 4, p. 477-490, 2002.

KIM, J.H., ET AL., A novel in vivo platform for studying alveolar bone regeneration in rat.Journal of tissue engineering, 2013. 4: p. 2041731413517705.

KURNIAWAN, Denni et al. Finite element analysis of bone–implant biomechanics: refinement through featuring various osseointegration conditions. International journal of oral and maxillofacial surgery, v. 41, n. 9, p. 1090-1096, 2012.

LEE, Cameron CY; JAGTAP, Rasika R.; DESHPANDE, Gaurav S. Longitudinal treatment of cleft lip and palate in developing countries: dentistry as part of a multidisciplinary endeavor. Journal of Craniofacial Surgery, v. 25, n. 5, p. 1626-1631, 2014.

LONG JR, Ross E.; SEMB, Gunvor; SHAW, William C. Orthodontic treatment of the patient with complete clefts of lip, alveolus, and palate: lessons of the past 60 years. The Cleft palate-craniofacial journal, v. 37, n. 6, p. 1-13, 2000.

LUQUE-MARTÍN, Estela; TOBELLA-CAMPS, María L.; RIVERA-BARÓ, Alejandro. Alveolar graft in the cleft lip and palate patient: review of 104 cases. Medicina oral, patologia oral y cirugia bucal, v. 19, n. 5, p. e531, 2014.

LUQUE-MARTÍN, Estela; TOBELLA-CAMPS, María L.; RIVERA-BARÓ, Alejandro. Alveolar graft in the cleft lip and palate patient: review of 104 cases. Medicina oral, patologia oral y cirugia bucal, v. 19, n. 5, p. e531, 2014.

MANDALUNIS, P. Remodelación ósea. Actualizaciones en Osteología, v. 2, n. 1, p. 16-18, 2006.

MISCH, Craig M. Autogenous bone: is it still the gold standard?. Implant dentistry, v. 19, n. 5, p. 361, 2010.

MOSSEY, Peter A. et al. Cleft lip and palate. The Lancet, v. 374, n. 9703, p. 1773-1785, 2009.

MÜLLER, Ralph; RÜEGSEGGER, P. Three-dimensional finite element modelling of non-invasively assessed trabecular bone structures. Medical engineering & physics, v. 17, n. 2, p. 126-133, 1995.

NAGASHIMA, Hayato et al. Evaluation of bone volume after secondary bone grafting in unilateral alveolar cleft using computer-aided engineering. The Cleft Palate-Craniofacial Journal, v. 51, n. 6, p. 665-668, 2014.

NGUYEN, P.D., ET AL., Establishment of a critical-sized alveolar defect in the rat: a model for human gengivoperiosteoplasty. Plastic and reconstructive surgery, 2009. 123(3): p. 817-25.

NORDIN, Margareta; FRANKEL, Victor Hirsch (Ed.). Basic biomechanics of the musculoskeletal system. Lippincott Williams & Wilkins, 2001.

OCHS, Mark W. Alveolar cleft bone grafting (Part II): secondary bone grafting. Journal of oral and maxillofacial surgery, v. 54, n. 1, p. 83-88, 1996.

OH, TAE SUK ET AL. Risk factor analysis of bone resorption following secondary alveolar bone grafting using three-dimensional computed tomography. Journal of Plastic, Reconstructive & Aesthetic Surgery, v. 69, n. 4, p. 487-492, 2016.

PEAMKAROONRATH, Chonthicha; GODFREY, Keith; CHATRCHAIWIWATANA, Supaporn. New clinical method for alveolar bone graft evaluation in cleft patients: a pilot study. The Cleft Palate-Craniofacial Journal, v. 48, n. 3, p. 286-292, 2011.

PINHEIRO, Antonio Luiz B.; GERBI, Marleny Elizabeth MM. Photoengineering of bone repair processes. Photomedicine and Laser Therapy, v. 24, n. 2, p. 169-178, 2006.

RALSTON, Stuart H. Bone structure and metabolism. Medicine, v. 45, n. 9, p. 560-564, 2017.

RAZI, Tahmineh; NIKNAMI, Mahdi; GHAZANI, Fakhri Alavi. Relationship between Hounsfield unit in CT scan and gray scale in CBCT. Journal of dental research, dental clinics, dental prospects, v. 8, n. 2, p. 107, 2014.

ROCHA, Roberto et al. Ideal treatment protocol for cleft lip and palate patient from mixed to permanent dentition. American Journal of Orthodontics and Dentofacial Orthopedics, v. 141, n. 4, p. S140-S148, 2012.

SAN CHEONG, Vee et al. Novel adaptive finite element algorithms to predict bone ingrowth in additive manufactured porous implants. Journal of the mechanical behavior of biomedical materials, v. 87, p. 230-239, 2018.

SCHMIDT, Andrew H. Autologous bone graft: Is it still the gold standard?. Injury, 2021.

SCHULTZE-MOSGAU, Stefan et al. Analysis of bone resorption after secondary alveolar cleft bone grafts before and after canine eruption in connection with orthodontic gap closure or prosthodontic treatment1. Journal of oral and maxillofacial surgery, v. 61, n. 11, p. 1245-1248, 2003.

SEIFELDIN, Sameh A. Is alveolar cleft reconstruction still controversial? (Review of literature). The Saudi dental journal, v. 28, n. 1, p. 3-11, 2016.

SEMB, Gunvor. Alveolar bone grafting. In: Cleft Lip and Palate. Karger Publishers, 2012. p. 124-136.

SHIROTA, T. et al. Analysis of bone volume using computer simulation system for secondary bone graft in alveolar cleft. International journal of oral and maxillofacial surgery, v. 39, n. 9, p. 904-908, 2010.

SHIROTA, T. et al. Analysis of bone volume using computer simulation system for secondary bone graft in alveolar cleft. International journal of oral and maxillofacial surgery, v. 39, n. 9, p. 904-908, 2010.

SILVA FILHO, Omar Gabriel da et al. Reconstruction of alveolar cleft with allogenous bone graft: clinical considerations. Dental press journal of orthodontics, v. 18, n. 6, p. 138-147, 2013.

SILVANA, R. et al. The effect of CCL3 and CCR1 in bone remodeling induced by mechanical loading during orthodontic tooth movement in mice. Bone, v. 52, n. 1, p. 259-267, 2013.

SIMMONS, Craig A.; MEGUID, Shaker A.; PILLIAR, Robert M. Differences in osseointegration rate due to implant surface geometry can be explained by local tissue strains. Journal of Orthopaedic Research, v. 19, n. 2, p. 187-194, 2001.

SINDET-PEDERSEN, Steen; ENEMARK, Hans. Comparative study of secondary and late secondary bone-grafting in patients with residual cleft defects. Short-term evaluation. International journal of oral surgery, v. 14, n. 5, p. 389-398, 1985.

SPINA, Victor. A proposed modification for the classification of cleft lip and cleft palate. The Cleft palate journal, v. 10, p. 251-252, 1973.

STOLTZ, Jean-François et al. Influence of mechanical forces on bone: introduction to mechanobiology and mechanical adaptation concept. Journal of Cellular Immunotherapy, v. 4, n. 1, p. 10-12, 2018.

SUN, Jian et al. Biological Effects of Orthodontic Tooth Movement Into the Grafted Alveolar Cleft. Journal of Oral and Maxillofacial Surgery, v. 76, n. 3, p. 605-615, 2018.

TAI, Chi-Chia E.; SUTHERLAND, I. Scott; MCFADDEN, Leland. Prospective analysis of secondary alveolar bone grafting using computed tomography. Journal of oral and maxillofacial surgery, v. 58, n. 11, p. 1241-1249, 2000.

TANAKA, Ricardo et al. Incorporação dos enxertos ósseos em bloco: processo biológico e considerações relevantes. ConScientiae Saúde, v. 7, n. 3, 2008.

TANNURE, Patricia Nivoloni et al. Prevalence of dental anomalies in nonsyndromic individuals with cleft lip and palate: a systematic review and meta-analysis. The Cleft Palate-Craniofacial Journal, v. 49, n. 2, p. 194-200, 2012.

THEREZA-BUSSOLARO, Claudine et al. Development, validation and application of a 3D printed model depicting adenoid hypertrophy in comparison to a Nasoendoscopy. Head & face medicine, v. 16, n. 1, p. 1-8, 2020.

TOKUGAWA, Yoshiyasu et al. Bone regeneration of canine artificial alveolar clefts using bone-marrow-derived mesenchymal stromal cells and β-tricalcium phosphate: A preliminary study. Orthodontic Waves, v. 71, n. 2, p. 51-58, 2012.

TROJAN-SERPE, Larissa Carvalho et al. Strain level at midpalatal suture-correlation with mechanobiological concepts. 22nd Int. Congr. Mech. Eng, p. 8523-8531, 2013.

UZEL, Aslıhan et al. The Effects of Maxillary Expansion on Late Alveolar Bone Grafting in Patients with Unilateral Cleft Lip and Palate. Journal of Oral and Maxillofacial Surgery, 2018.

VÉLEZ MURIEL, Sandra Melisa. Estudio computacional del efecto de cargas mecánicas en el comportamiento biomecánico de un injerto alveolar. Tesis de Maestría en Ingeniería Mecánica, 2020.

WHITE, Stuart C.; PHAROAH, Michael J. Oral radiology-E-Book: Principles and interpretation. Elsevier Health Sciences, 2014.

WU, Ziran; ROBINSON, John. Edge-preserving colour-to-greyscale conversion. IET Image Processing, v. 8, n. 4, p. 252, 2014.

YANG, Chenjie et al. Study on Tooth Movement After the Alveolar Bone Grafting in Patients With Unilateral Cleft Lip and Palate. The Journal of craniofacial surgery, 2019.

Annex I

UNIVERSIDADE FEDERAL DE MINAS GERAIS

CEUA
COMISSÃO DE ÉTICA NO USO DE ANIMAIS

Prezado(a):

Esta é uma mensagem automática do sistema Solicite CEUA que indica mudança na situação de uma solicitação.

Protocolo CEUA: 338/2017
Título do projeto: Avaliação do enxerto ósseo secundário durante a movimentação dentária ortodôntica em modelo experimental animal.
Finalidade: Pesquisa
Pesquisador responsável: Soraia Macari
Unidade: Faculdade de Odontologia
Departamento: Departamento de Odontopediatria e Ortodontia

Situação atual: Decisão Final - Aprovado

Aprovado na reunião do dia 04/12/2017. Validade: 04/12/2017 à 03/12/2022

Belo Horizonte, 04/12/2017.

Atenciosamente,

Sistema Solicite CEUA UFMG
https://aplicativos.ufmg.br/solicite_ceua/

Universidade Federal de Minas Gerais
Avenida Antônio Carlos, 6627 – Campus Pampulha
Unidade Administrativa II – 2º Andar, Sala 2005
31270-901 – Belo Horizonte, MG – Brasil
Telefone: (31) 3409-4516
www.ufmg.br/bioetica/ceua - cetea@prpq.ufmg.br
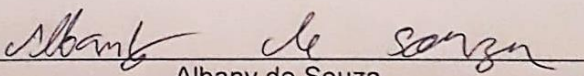
Annex II

TERMO DE CESSÃO DE DIREITO DE USO DE IMAGEM E DIREITOS

PATRIMONIAIS PARA FINS CIENTÍFICOS

Eu, Albany de Souza, nacionalidade brasileiro, estado civil solteiro, profissão de jardineiro, inscrito no CPF sob o nº 10556541600 e RG sob o nº 15059570 , autorizo o uso da minha imagem e da imagem de minha documentação ortodôntica (radiografias, fotos, modelos e tomografias) para fins de divulgação e publicidade do trabalho de pesquisa, "Avaliação do Enxerto ósseo no paciente com fenda palatina", bem assim a cessão de todo e qualquer direito autoral patrimonial resultante de eventuais produtos decorrentes desta pesquisa, nos termos do art. 111 da Lei nº 8.666/1993.

Belo Horizonte, 10 de outubro de 2014.

_____
Albany de Souza